

**The Development of an Analytical Model for the  
KODAK DIGITAL SCIENCE™ Color Infrared Cameras  
and Its Aerial Imaging Applications**

**Imaging Science MS Project  
Todd Birdsall  
Summer, 1997**

**Acknowledgments:**

I would like to acknowledge and thank the following people for their support on this project :

Dr. John Schott, Professor, Director, Digital Image & Remote Sensing Laboratory, RIT  
- Overall project advisor

Mr. Rolando Raqueño, Associate Scientist, RIT  
- Weekly technical direction and support

Mr. John Newman, Senior System Engineer, Eastman Kodak Company  
- Color science technical advice

Mr. Mark Shrader, Senior Development Engineer, Eastman Kodak Company  
- Camera software driver technical advice

**Dedication:**

This paper is dedicated to my loving wife, Debbie, and to my two great kids, Holly and Troy. My family has inspired and supported me throughout my academic career at RIT.

**Abstract:**

The new KODAK DIGITAL SCIENCE™ Color Infrared Cameras provide an affordable, high-resolution digital imaging solution for many low-altitude remote sensing applications. These remote sensing applications span forest management, law enforcement, environmental monitoring and agriculture crop analysis. This paper describes the technical aspects of the color infrared (CIR) cameras, and an analytical model of the cameras in aerial imaging scenarios. The model is based on physical attributes of the imaging chain and incorporates Modtran atmospheric data, measured ground target reflectance data, predicted aircraft motion, and measured/computed camera characteristics. It is capable of predicting both radiometric and image quality performance of a complete aerial image chain. Output data is in terms of 8-bit digital counts for the radiometric computations and ground resolving distance (GRD) for image quality analysis. Normalized difference vegetation index (NDVI), for agriculture analysis, is also computed. The model is flexible and robust enough to predict overall system performance in real life imaging scenarios or to be used as a design tool for camera optimization.

# Table of Contents

<b>1.0 BACKGROUND.....</b>	<b>1</b>
1.1 CIR CAMERA OVERVIEW.....	1
1.2 MODEL OVERVIEW.....	3
<b>2.0 APPROACH.....</b>	<b>4</b>
<b>3.0 TECHNICAL DESCRIPTION.....</b>	<b>6</b>
3.1 COLOR INFRARED CAMERA.....	6
3.2 MODEL DESCRIPTION.....	10
3.2.1 ATMOSPHERIC SECTION.....	10
3.2.2 GROUND TARGET SECTION.....	13
3.2.3 CAMERA SECTION.....	16
3.2.4 RADIOMETRIC MODEL EQUATIONS.....	19
3.2.5 IMAGE QUALITY MODEL EQUATIONS.....	24
<b>4.0 RESULTS.....</b>	<b>30</b>
4.1 FLIGHT TEST DATA.....	30
4.2 MODELING CASE STUDY - THREE WHEAT CURVES.....	31
<b>5.0 CONCLUSION / SUMMARY.....</b>	<b>35</b>
<b>6.0 APPENDIX.....</b>	<b>37</b>
APPENDIX 1 - FLIGHT TEST IMAGE.....	38
APPENDIX 2 - NDVI IMAGE OF THE FLIGHT TEST IMAGE.....	40
APPENDIX 3 - RADIOMETRIC MODEL SAMPLE RUN.....	42
APPENDIX 4 - IMAGE QUALITY MODEL SAMPLE RUN.....	59
APPENDIX 5 - IMAGE PROCESSING DIAGRAM.....	70
<b>7.0 REFERENCES.....</b>	<b>72</b>

## List of Figures

FIGURE 1: SOLAR ENERGY PATH IN THE IMAGING CHAIN.....	4
FIGURE 2: CCD SPECTRAL RESPONSE PLOT.....	6
FIGURE 3: COLOR FILTER ARRAY (CFA) MADE BY KODAK.....	7
FIGURE 4: COLOR FILTER ARRAY NORMALIZED TRANSMITTANCE PLOT .....	7
FIGURE 5: INFRARED CAPTURE .....	8
FIGURE 6: BAND-PASS FILTER TRANSMITTANCE PLOT.....	9
FIGURE 7: EXOATMOSPHERIC SPECTRAL IRRADIANCE PLOT.....	10
FIGURE 8: DOWNWELLED SOLAR RADIANCE PLOT .....	11
FIGURE 9: UPWELLED SOLAR RADIANCE PLOT.....	11
FIGURE 10: SUN TO TARGET ATMOSPHERIC TRANSMITTANCE PLOT.....	12
FIGURE 11: TARGET TO SENSOR ATMOSPHERIC TRANSMITTANCE PLOT .....	12
FIGURE 12: MACBETH COLORCHECKER CHART ROW #1 REFLECTANCE PLOT.....	13
FIGURE 13: MACBETH COLORCHECKER CHART ROW #2 REFLECTANCE PLOT.....	14
FIGURE 14: MACBETH COLORCHECKER CHART ROW #3 REFLECTANCE PLOT.....	14
FIGURE 15: MACBETH COLORCHECKER CHART ROW#4 REFLECTANCE PLOT .....	15
FIGURE 16: WHEAT REFLECTANCE PLOT.....	15
FIGURE 17: 28 MM NIKON LENS TRANSMITTANCE PLOT.....	16
FIGURE 18: 28 MM LENS FALL-OFF PLOT.....	17
FIGURE 19: LENS MTF PLOT .....	17
FIGURE 20: COLOR INTERPOLATION MTF PLOT .....	18
FIGURE 21: AIRCRAFT MOTION MTF FOR VARIOUS INTEGRATION TIMES PLOT.....	25
FIGURE 22: AIRCRAFT MOTION MTF FOR VARIOUS AIRCRAFT SPEEDS PLOT .....	26
FIGURE 23: AIRCRAFT MOTION MTF FOR VARIOUS AIRCRAFT ALTITUDES PLOT .....	26
FIGURE 24: DRIVER COMPARISON PLOT .....	30
FIGURE 25: THE CIR CAMERA IMAGE PROCESSING DIAGRAM .....	71

## List of Tables

TABLE 1: WHEAT DIFFERENTIATION.....	31
TABLE 2: LENS FALL-OFF AFFECT ON NDVI PREDICTIONS.....	32
TABLE 3: ATMOSPHERIC IMPACT ON NDVI PREDICTIONS .....	33
TABLE 4: WHEAT CASE-STUDY IMAGE QUALITY SUMMARY .....	34

## 1.0 Background

### 1.1 CIR Camera Overview

The utilization of traditional infrared film photography for various applications has been well documented in many publications. Key current applications include forest management, law enforcement, environmental monitoring and agriculture crop analysis.

The KODAK DIGITAL SCIENCE™ Color Infrared Digital Cameras provide the benefits of infrared film along with a multitude of digital imaging benefits. Kodak currently offers two models of the infrared cameras. The KODAK DIGITAL SCIENCE™ 420 Color Infrared Camera and KODAK DIGITAL SCIENCE™ 460 Color Infrared Camera. The major difference between the two camera models is the size of the CCD imager. The 420 model has a 1.5 million pixel array incorporated into it while the 460 model utilizes a 6 million pixel imager.

The CIR digital cameras are not intended to replace the current 9 inch x 9 inch aerial infrared mapping films. The mapping films have superior resolution and orders of magnitude more area coverage capabilities than the current CIR cameras. For example, if a 9 inch x 9 inch piece of film was scanned at 9  $\mu\text{m}$  x 9  $\mu\text{m}$  pixel pitch with a dynamic range of 8 bits per color, the resulting image file size would be 1.9 GB. This is over 100 times larger than the image files from the 460 CIR camera. The 460 model produces a final file size of 18 MB per image.

The CIR camera and the infrared film essentially have the same spectral response. The spectral response of the CIR camera is slightly broader than the infrared film. The camera, with its silicon CCD, is sensitive from 400 nanometers (nm) to 1000 nm. The film's sensitivity falls between 400-900 nm. The 100 nm difference from 900 nm to 1000 nm is trivial for most aerial applications because of the H<sub>2</sub>O absorption band in the atmosphere of between 900 nm and 1000 nm.

The benefits of the CIR cameras lies in their ability to produce reliable, repeatable images in a fraction of the time it would take to get the same results from traditional film. The output images from the digital camera are essentially instant. Some aerial photographers use the camera in conjunction with an on-board computer and view the imagery in-flight. The imagery from the CIR cameras are very consistent under the same capture conditions. This fact gives rise to the possibility of using the cameras as a radiometer for some remote sensing applications. In comparison, film radiometry is very difficult because of its roll-to-roll sensitometric variations.

A major revolution in remote sensing imagery is taking place. Over the next few years, electro-optical (E-O), multispectral high-resolution, commercial satellite imagery will be readily available to everyone. Currently, there is multispectral (MS) imagery available from satellite systems like Landsat and Spot. These systems produce MS imagery at 30 meter and 10 meter ground sample distance (GSD), respectively. Soon to be launched are high-resolution satellite systems like Space Imaging and EarthWatch. Both systems will provide MS imagery at 4 meter GSD.

There is no question that the new imaging satellites will compete with the aerial photography industry. The questions that still remains is how much, and how fast? Satellites have inherent system constraints that impact their ability to capture acceptable results. Some of the system constraints that must be considered include resolution, cloud-covered targets, and target revisit time. The new breed of commercial satellites will be resolution limited, by law, to 1 meter panchromatic GSD and 4 meter MS GSD or less. With this GSD constraint, objects smaller than 2 meters will not be resolvable. The new commercial E-O satellites have two other major limitations. First, they cannot image targets that are cloud covered. This means land mass that is primarily cloud covered will not be imaged by satellites very often. Secondly, satellites fly in specific elliptical orbits, which affects their ability to revisit specific targets at a specific resolution periodically. Targets will only be in view for a very short time, and only once a month or longer, until more satellites are deployed.

Aerial photography is not limited by these satellite constraints. Aircraft can achieve greater than 1 meter GSD. Depending on the urgency of the imagery, aircraft can fly under clouds and acquire images. Aircraft can fly over a target at the same resolution as necessary. This is a requirement for such applications as emergency rescue operations and some crop analysis projects.

## **1.2 Model Overview**

The need for accurately predicting overall system performance is a must for today's imaging systems. No performance prediction model of the CIR camera exists. Also, there is no CIR camera optimization tool addressing the entire image chain. This paper presents an analytical CIR camera model that embodies the entire aerial imaging chain.

The focus of this paper is a detailed description of the model. In section 2, the approach of the model is presented. Section 3 is a technical description of all of the imaging chain components of the model and their interactions. Section 4 provides results of a modeling case study. The case study utilized three temporal states of wheat to show the robustness of the model and the CIR camera. Also, output imagery of the camera is presented in empirical form. In section 5, conclusions, summaries and possible follow-on work is presented.



## 2.0 Approach

A systems approach to model the physical attributes of each part of the imaging chain has been adopted. The atmosphere, ground target, aircraft, CIR camera, and digital image processing (Adobe Photoshop plug-in drivers) make up the major components of the imaging chain in the model. The model consists of two separate spreadsheets. One spreadsheet predicts the 8-bit digital count output of the camera's radiometric response in the imaging chain. The second spreadsheet estimates image quality of the camera's output in the imaging chain. In order to make the model as accurate as possible, measured data was used when available. Such data includes target reflectance data, filter and lens performance data, and CCD responsivity data. The details of the measured data are presented in section 3.

The radiometric model uses only reflected energy (no self-emission energy) throughout the imaging chain. Figure 1 depicts the solar energy path, as modeled in the radiometric model. Solar-ray "A" represents the exoatmospheric spectral irradiance. Solar-ray "B" represents the downwelled solar radiance. Solar-ray "C" represents the upwelled solar radiance<sup>13</sup>.

The atmosphere is modeled by incorporating Modtran data into it. The model assumes a lambertian (no angular dependence) ground target and no spectral shift with a change in solar zenith angle. Output of the radiometric analysis is in terms of 8-bit digital counts for a particular pixel.

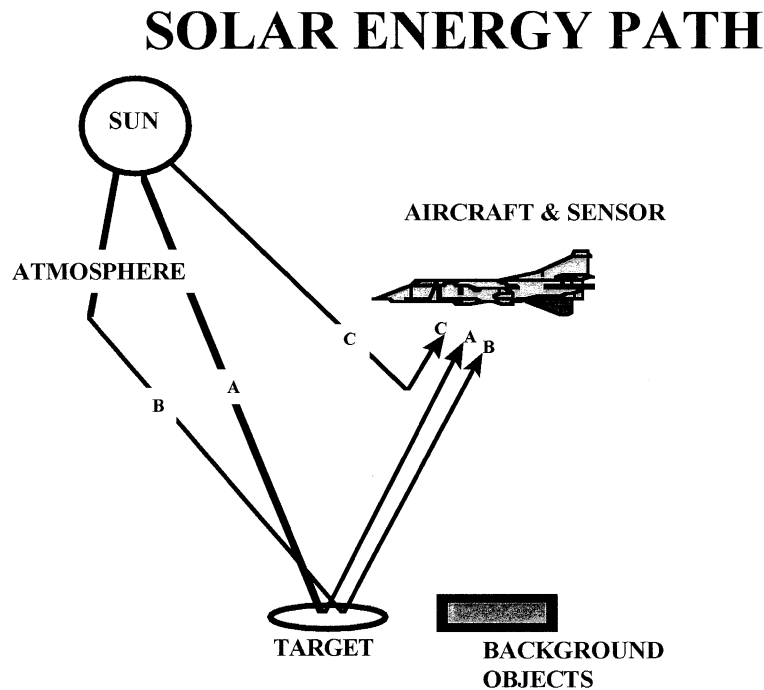


Figure 1: Solar Energy Path in the Imaging Chain

The image quality model is based on threshold modulation analysis (TMA)<sup>9</sup>. TMA compares the input or available modulation (ITM) to the required or needed modulation (TM) to predict an overall performance. The comparison between the input and required modulations can take place at any part in the imaging chain. The image quality model compares the two modulations at the focal plane. The image quality model uses data computed from the radiometric model (signal electrons, noise electrons, and the NDVI) as input for the noise modulation and target contrast calculations. The model assumes a linear system such that individual modulation transfer functions (MTF) can be cascaded together to predict overall input and required ITM. Both in-track and cross-track MTFs are computed and analyzed. The final output of the image quality portion is ground resolving distance (GRD) for a specific colored pixel.

### 3.0 Technical Description

#### 3.1 Color Infrared Camera

The color infrared cameras are derivatives of the KODAK PROFESSIONAL DCS Digital Cameras. Both the CIR and the Professional DCS cameras have silicon CCDs. To achieve three-channel information, the CCDs utilize a color filter array (CFA), "Bayer pattern" design<sup>1,3,8</sup>. The CFA protocol is 25% of the total pixels are red, 50% are green, and 25% are blue. Like most silicon CCDs, the Kodak cameras' CCDs are responsive from 400 nm to 1000 nm. The quantum efficiency (QE) curve of the 460 model's CCD is shown below in Figure 2.<sup>6</sup>

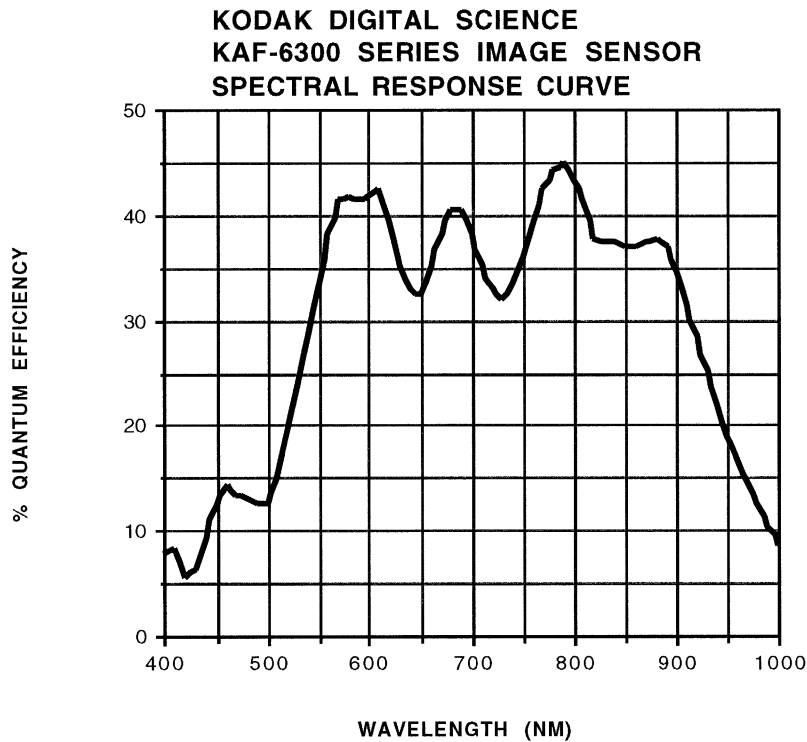


**Figure 2: CCD Spectral Response Plot**

The QE for the 420 camera is essentially the same. The Bayer pattern CFA of the CCD for the 460 camera is shown below in Figure 3.<sup>8</sup>

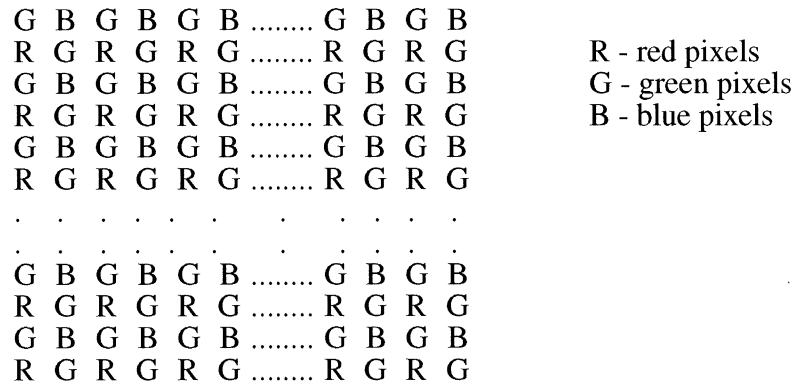


**Figure 3: Color Filter Array (CFA) made by KODAK**

As shown in Figure 4, the unique dye layers of the CFA are not only transmissive in their respective color-band, but also in the near-infrared region. It is this transmissive fact that makes the CIR version of the cameras possible. Note these curves are normalized to 80% peak in the model.

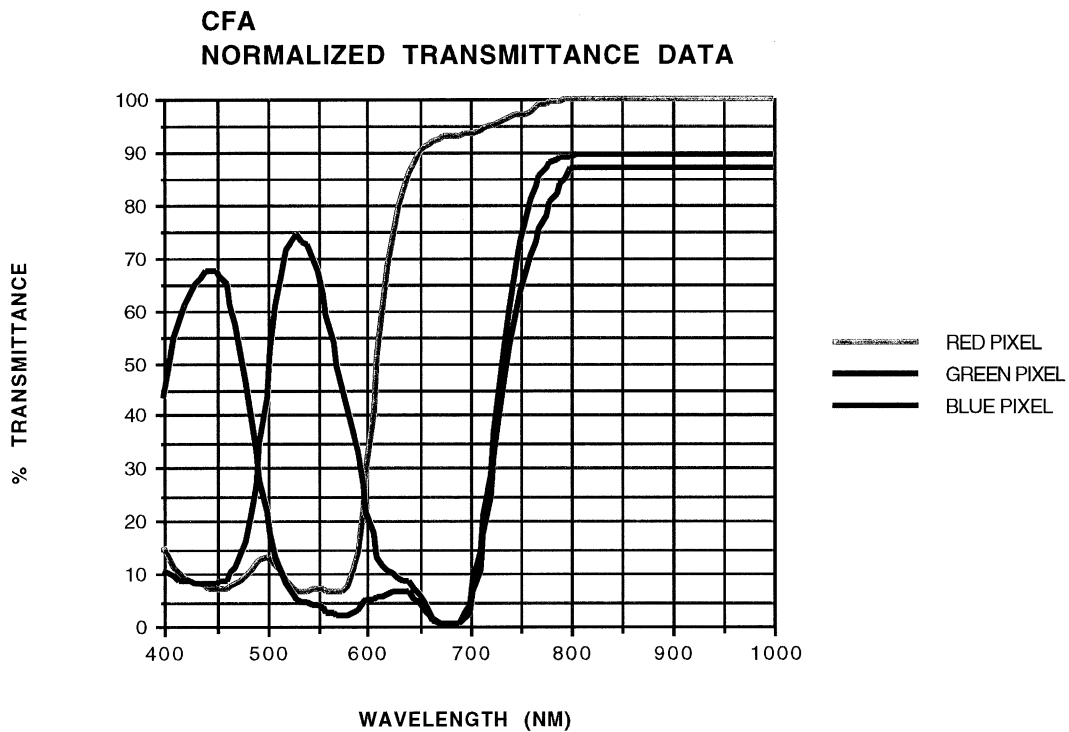


**Figure 4: Color Filter Array Normalized Transmittance Plot**

## Color Infrared Capture

The diagram below illustrates the entire color infrared capturing process.

# INFRARED CAPTURE

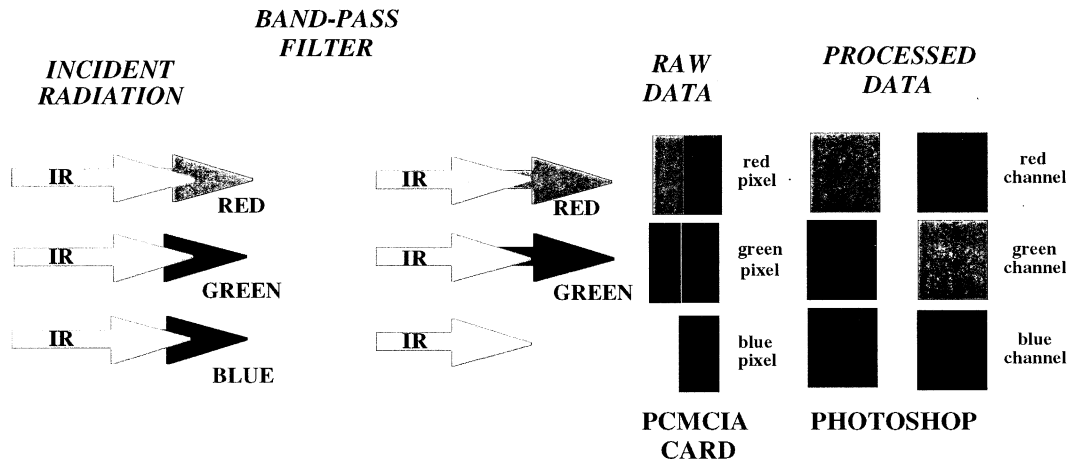
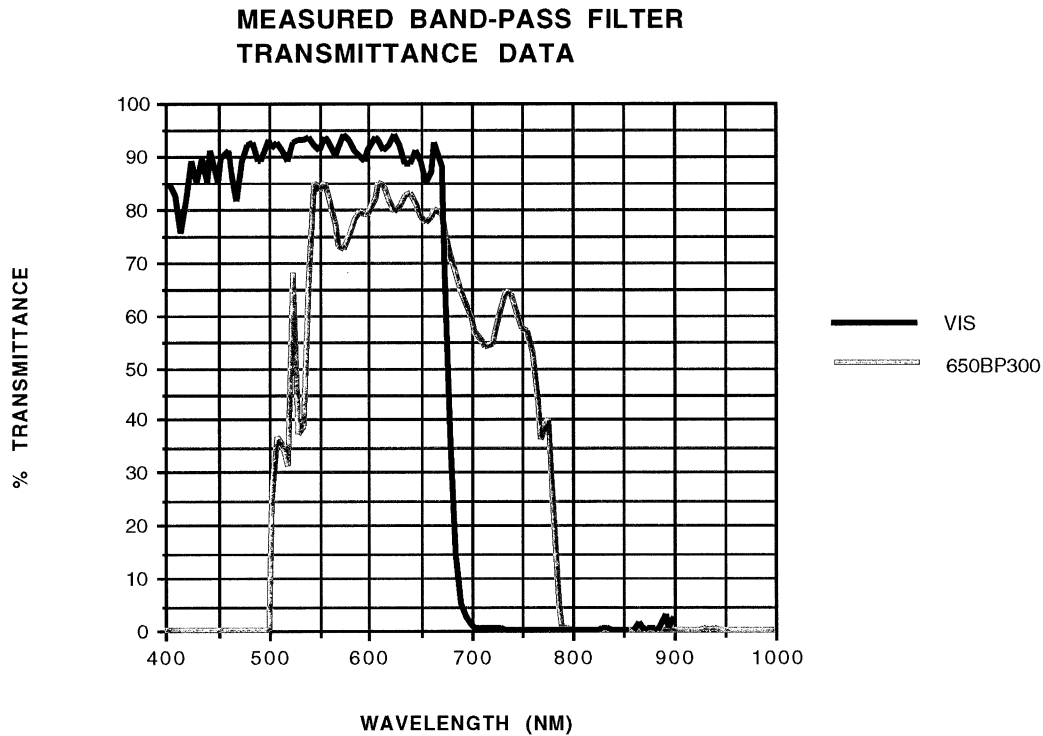


Figure 5: Infrared Capture

In order to use the CFA to capture near-infrared radiation, three major differences between the CIR and the generic Professional DCS cameras are required. These differences include the cover-glass on the charge coupled device (CCD), the lens band-pass filters, and image-processing software used to view the images. The CIR cameras are manufactured with a so-called clear cover glass, which allows infrared radiation to penetrate to the collecting portion of the CCD. The Professional DCS camera versions have IR attenuating cover glass on it.

The CIR cameras come with two distinct band-pass filters that screw on the front of the Nikon lenses.<sup>6</sup> The 650BP300 is used for near-infrared imaging and has a band-pass from 500 nm to 800 nm. The VIS filter is used to acquire natural color images from the CIR camera. Figure 6 shows the measured transmittance of the two CIR camera filters.



**Figure 6: Band-pass Filter Transmittance Plot**

The last major camera difference is found in the image-processing software. Both camera versions' software interpolates the raw color data to effectively give each pixel in the final image full, 24-bit color. In addition to the interpolation algorithms, the CIR driver backs-out the IR signal from the total signal captured by the red and green pixels, performs a color balance, and applies a false color registration. Therefore, the final infrared RGB image in file has the infrared signal in the red channel, the red signal in the green channel, and the green signal in the blue channel. This false color reassignment is the same assignment found in infrared film.

#### *CIR Camera Specifications<sup>6</sup>*

The following is a summary of the key CIR camera specifications:

Camera Body:	Nikon N90
Pixel Size:	9 $\mu\text{m}$ x 9 $\mu\text{m}$
Resolution( in pixel):	1012 x 1525 (420 model); 2056 x 3060 (460 model)
Spectral sensitivity:	400 nm - 1000 nm (no Filter) 400 nm - 700 nm (with VIS Filter) 500 nm - 800 nm (with IR Filter)
Dynamic Range:	36-bit color capture; 24-bit color stored
File Size:	4.5 MB (420 model); 18 MB (460 model)

## 3.2 Model Description

### 3.2.1 Atmospheric Section

Currently, the model has three different atmospheric options incorporated into it. All of the atmospheres have been generated using the USAF Modtran atmospheric model. Currently, the radiometric model's atmospheric options, are all Northeastern United States summer day models. The difference between the atmospheres is the amount of overcast and humidity in them. The three atmospheres are:

- 1) Clear summer day with 23 km visibility (Roch-23)
- 2) Summer day with 7 km visibility (Roch-7)
- 3) Summer day with only 5 km visibility and an additional 50% humidity added (Roch-5+).

The following five figures are plots of the Modtran out data from the three different atmospheres runs. Figure 7 is a plot of the three atmospheres exoatmospheric spectral irradiance. Figure 8 shows the downwelled solar radiance for the atmospheres. Figure 9 shows the upwelled solar radiance. Figures 10 and 11 are the atmospheric transmittance plots for the three atmospheres. Figure 10 displays the sun to target atmospheric transmittance and Figure 11 displays the target to sensor atmospheric transmittance.

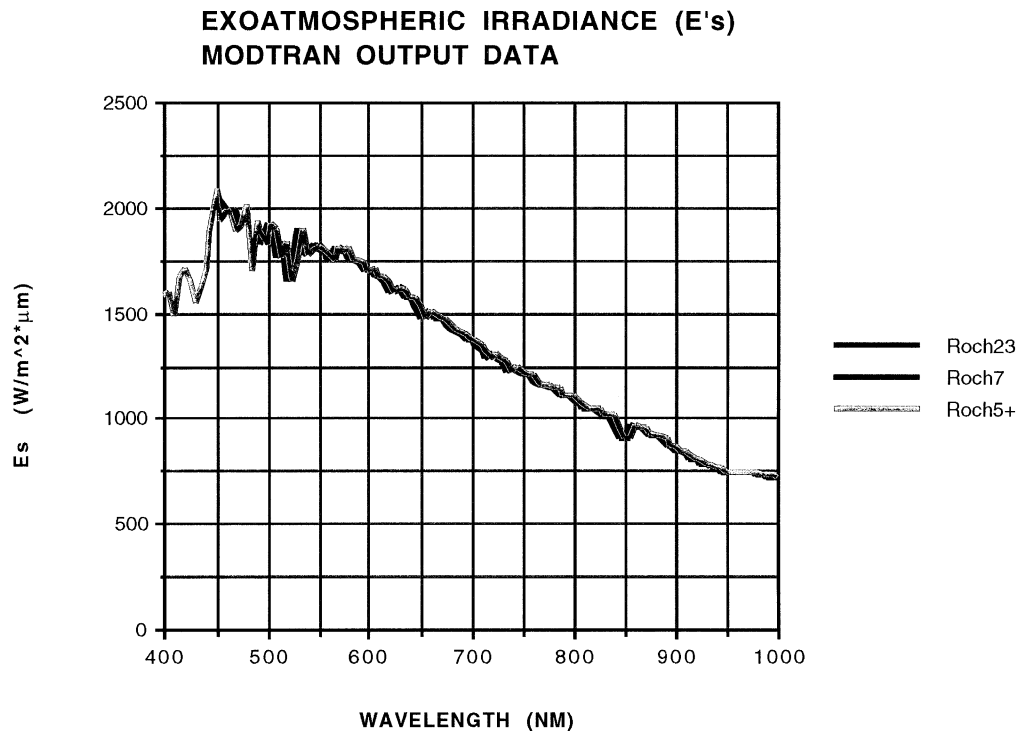


**Figure 7: Exoatmospheric Spectral Irradiance Plot**

**DOWNWELLED SOLAR RADIANCE (Ld)  
MODTRAN OUTPUT DATA**

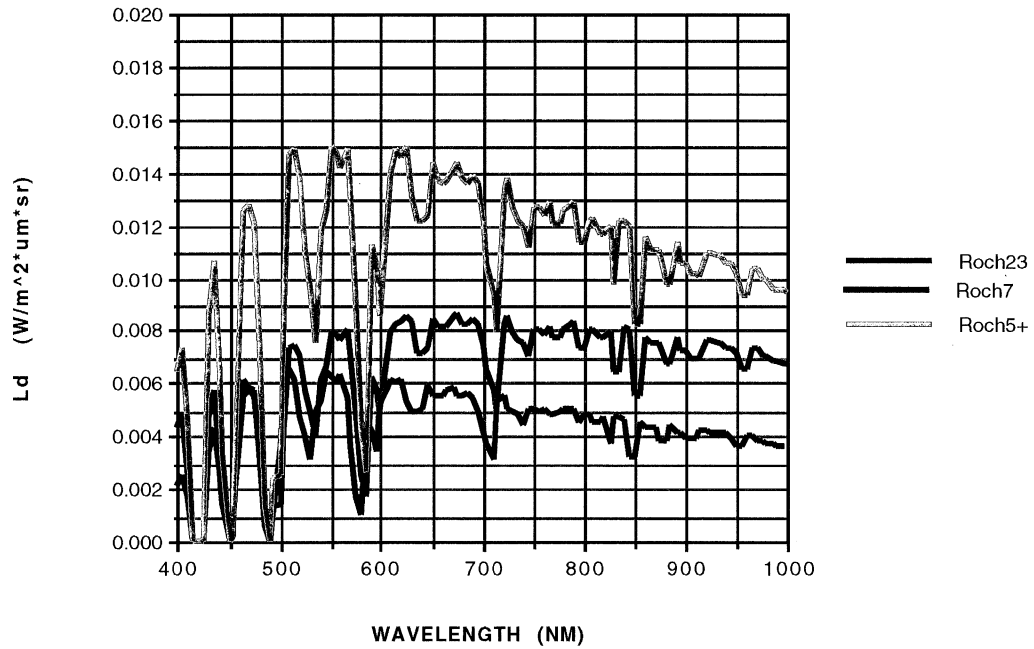


**Figure 8: Downwelled Solar Radiance Plot**

**UPWELLED SOLAR RADIANCE (Lu)  
MODTRAN OUTPUT DATA**

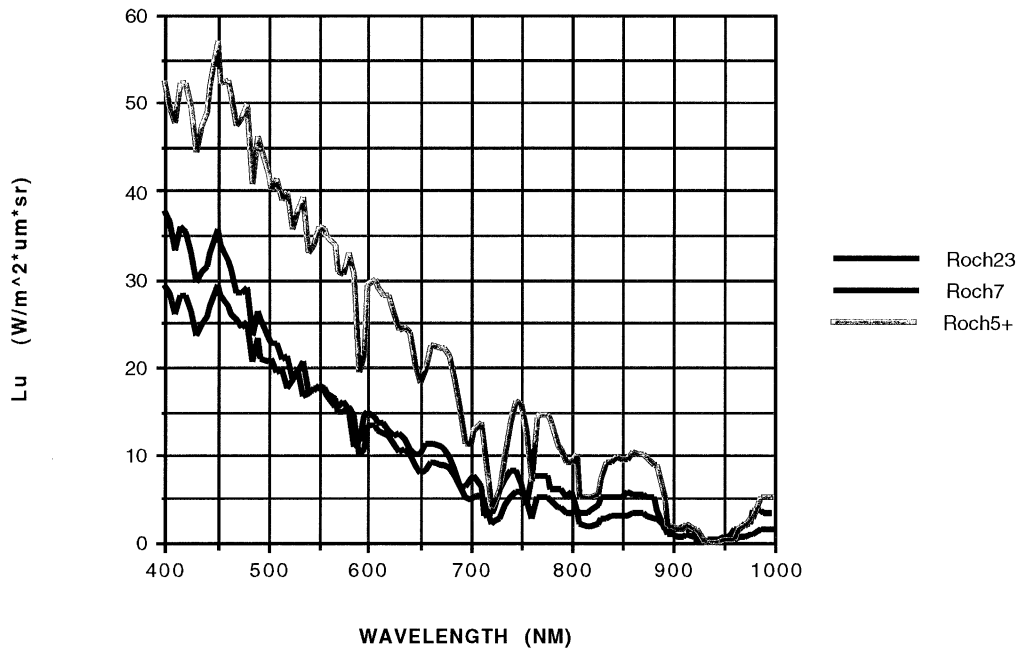


**Figure 9: Upwelled Solar Radiance Plot**



SUN TO TARGET ATMOS. TRANS. (T1)  
MODTRAN OUTPUT DATA

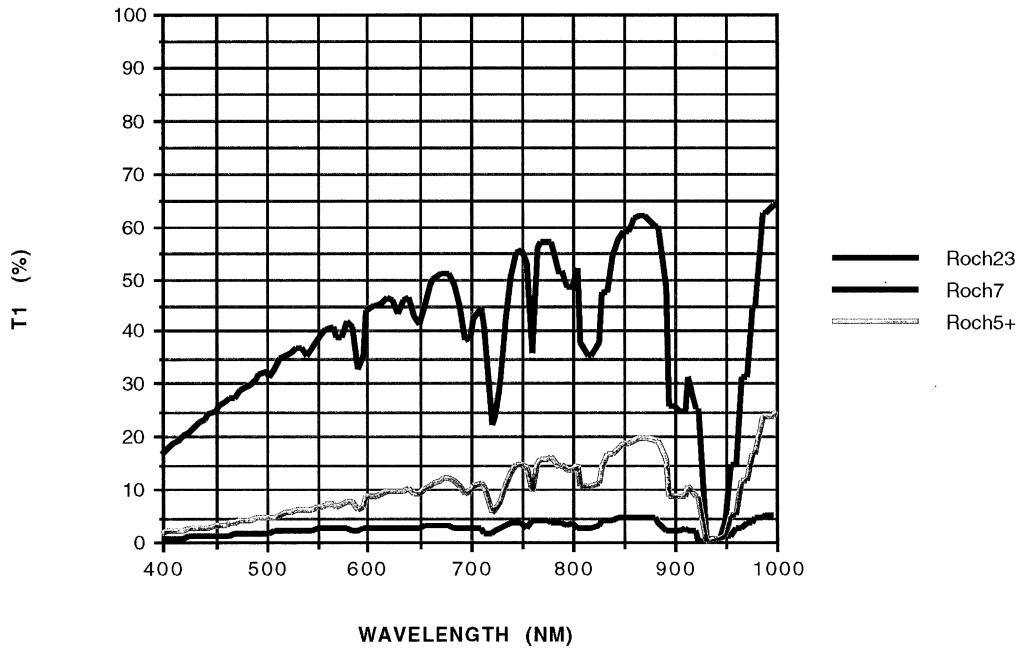


Figure 10: Sun to Target Atmospheric Transmittance Plot

TARGET TO SENSOR ATMOS TRANS. (T2)  
MODTRAN OUTPUT DATA

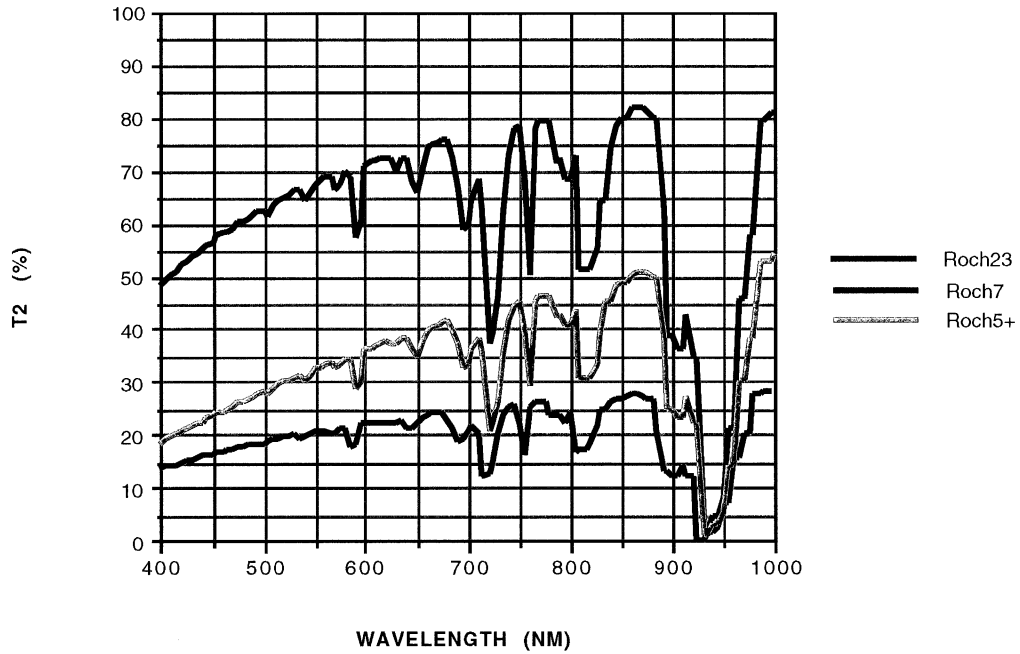
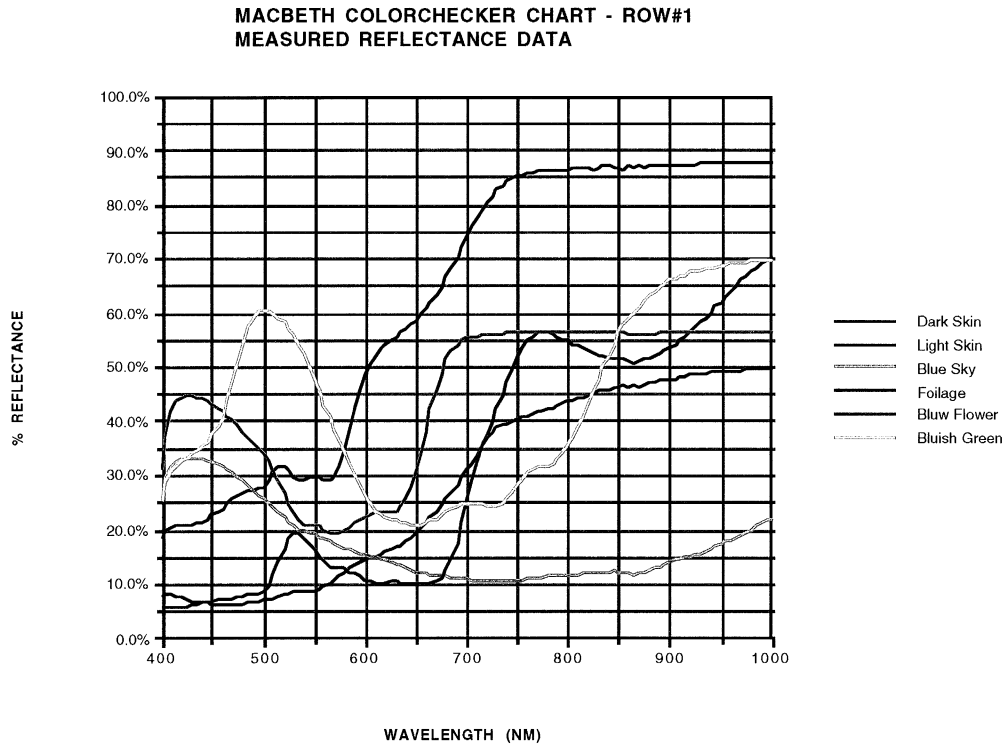


Figure 11: Target to Sensor Atmospheric Transmittance Plot

### 3.2.2 Ground Target Section

The model currently incorporates two main target source options, one man-made target and one natural target. The two targets are the Macbeth Colorchecker chart and Wheat reflectance data. The spectral reflectances of the targets were accurately measured between 400 nm and 1000 nm at 5 nm increments.

The Macbeth color checker is a well-known color standard used in the graphic arts and publishing industry. The Colorchecker consists of twenty-four different color patches. The patches consist of both a variety of colors and neutral gray levels. The Colorchecker typically comes in an oversize of 9 by 13 inches with individual patches of 1.75 by 1.75 inches. In 1996, Kodak contracted Macbeth to create a Colorchecker that has 1 meter by 1 meter size color patches and 2 meter by 2 meter gray patches. This mammoth version of the Colorchecker is for ground-truth analysis for aerial imaging. Figures 12 through 15 show the measured reflectances of the various patches.



**Figure 12: Macbeth Colorchecker Chart Row #1 Reflectance Plot**

MACBETH COLORCHECKER CHART - ROW #2  
MEASURED REFLECTANCE DATA

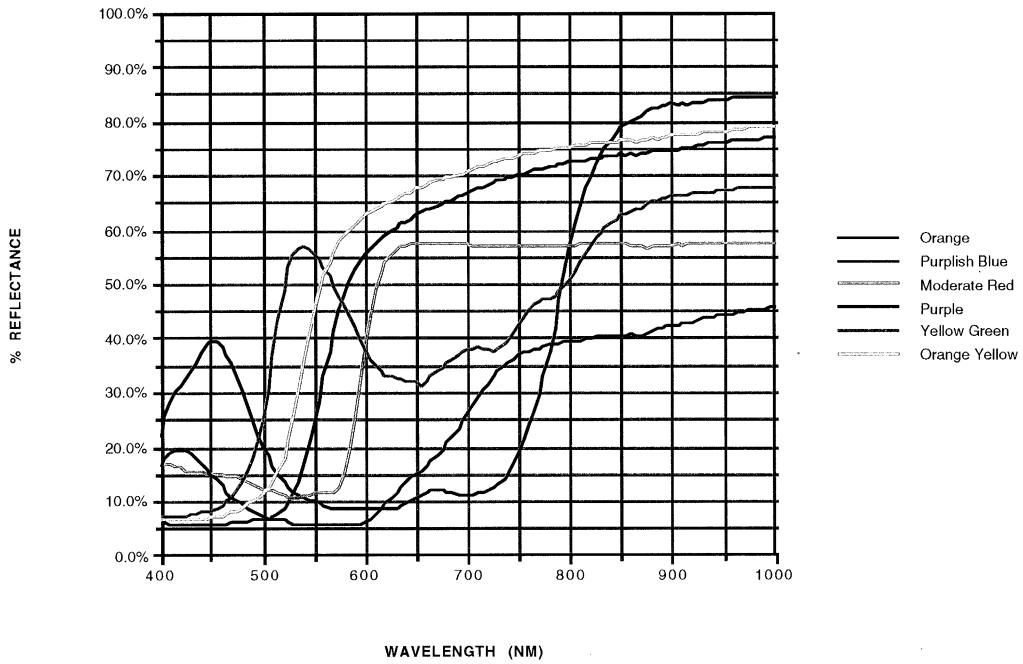


Figure 13: Macbeth Colorchecker Chart Row #2 Reflectance Plot

MACBETH COLORCHECKER CHART - ROW #3  
MEASURED REFLECTANCE DATA

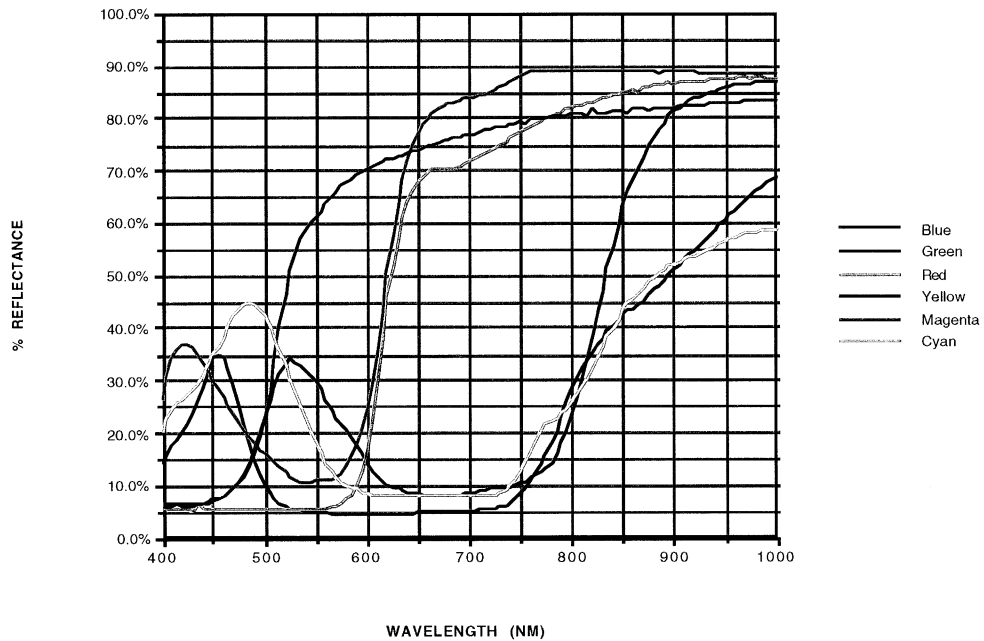
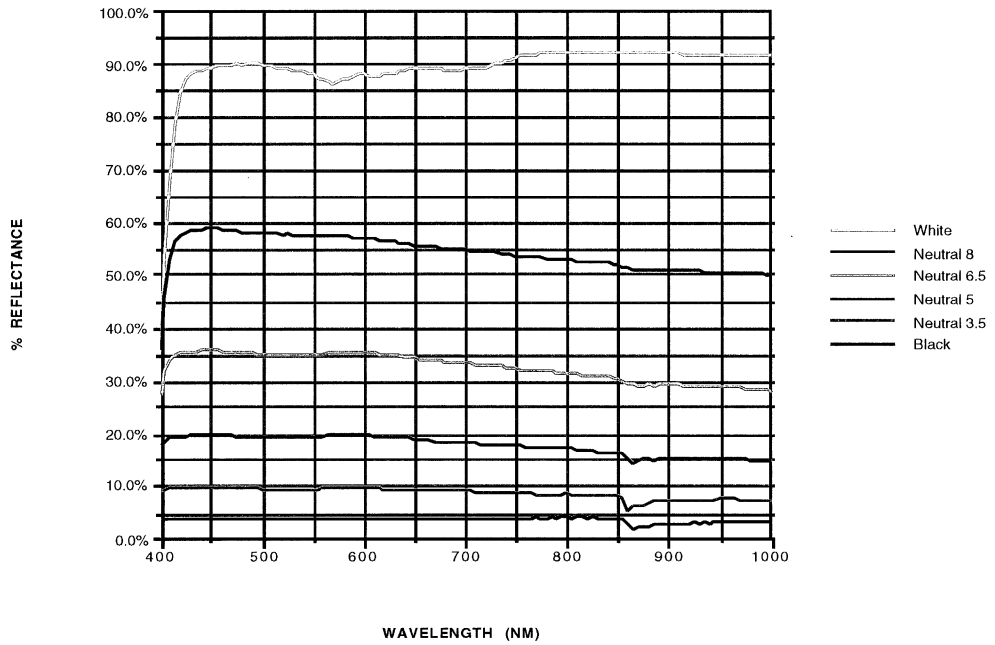


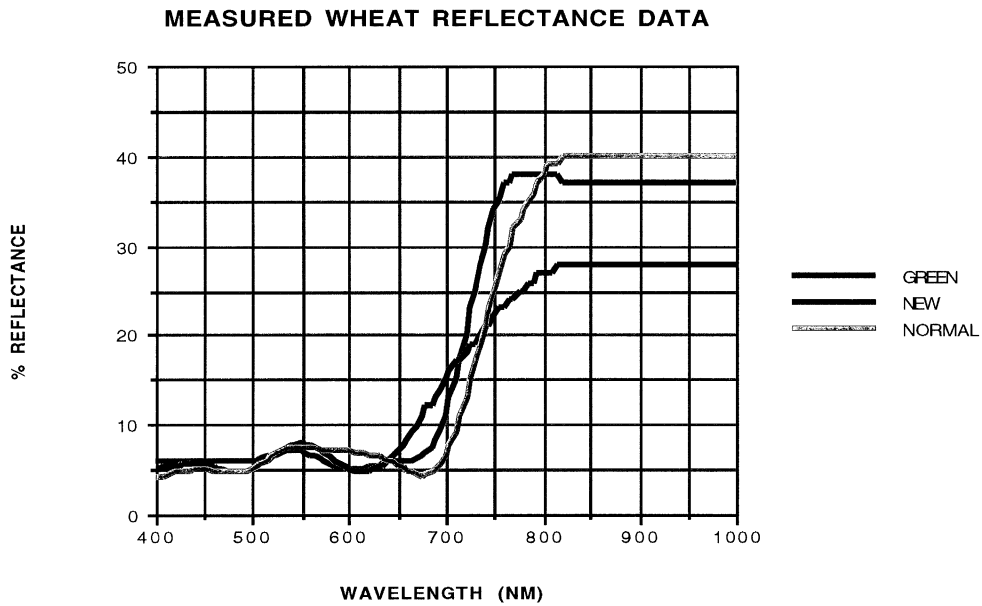
Figure 14: Macbeth Colorchecker Chart Row #3 Reflectance Plot

**MACBETH COLORCHECKER CHART - ROW #4  
MEASURED REFLECTANCE DATA**



**Figure 15: Macbeth Colorchecker Chart Row #4 Reflectance Plot**

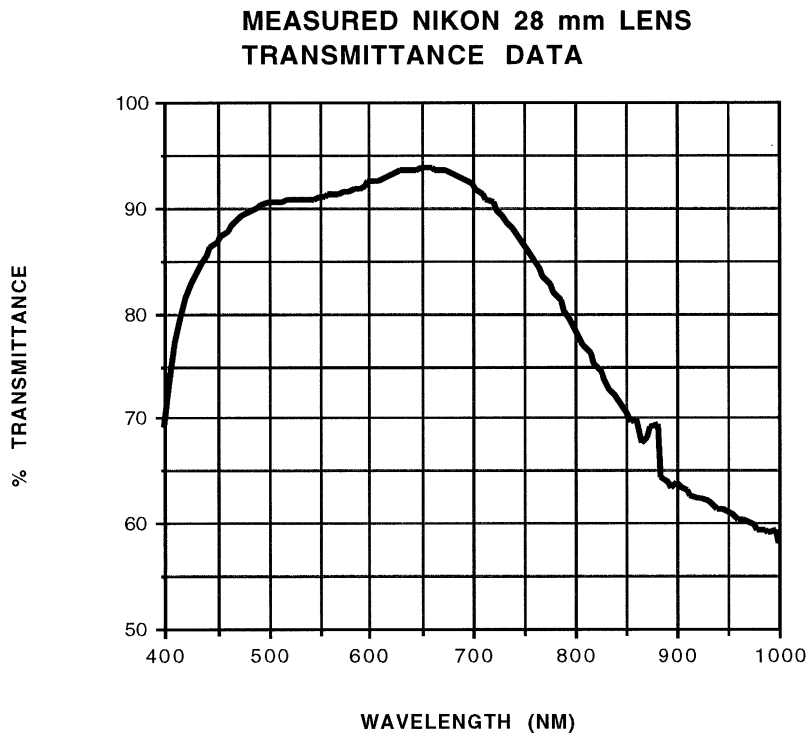
The second target spectra, measured wheat reflectance data, is composed of three stages of annual wheat growth. The reflectance curves of the three stages of growth are shown below in Figure 16.



**Figure 16: Wheat Reflectance Plot**

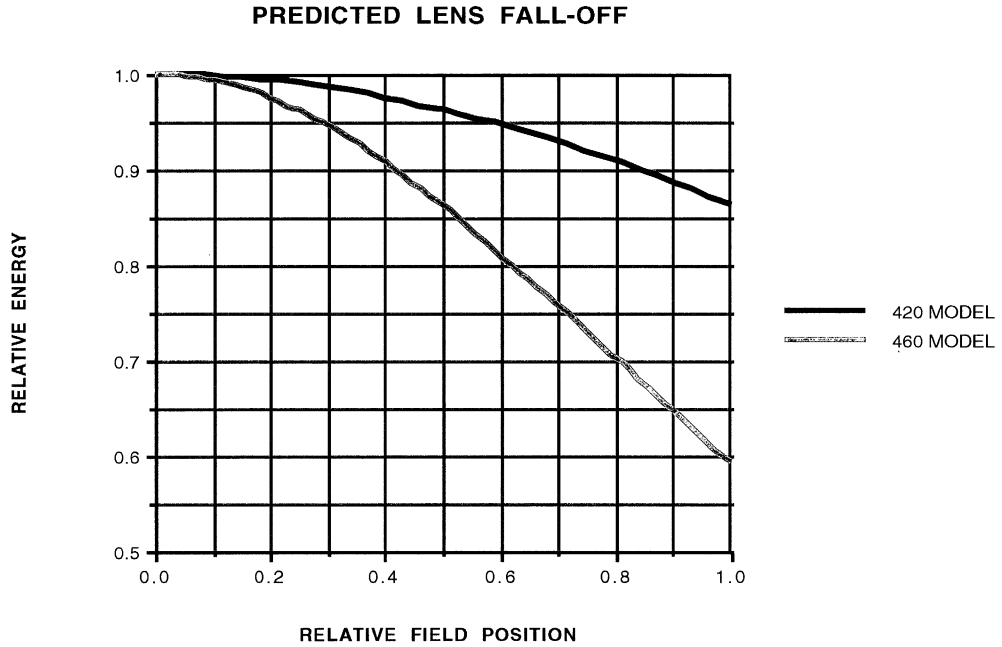
### 3.2.3 Camera Section

The major technical characteristics of the CIR cameras have already been discussed. For completeness, a few remaining radiometric modeling considerations of the camera must still be addressed. The transmittance of the camera's lens must be incorporated into the radiometric model. The spectral transmittance of a 28 mm Nikon Nikkor lens was measured, and the data is shown in Figure 17 below. (Note, the anomaly around 875 nm is due to the spectrometer.)



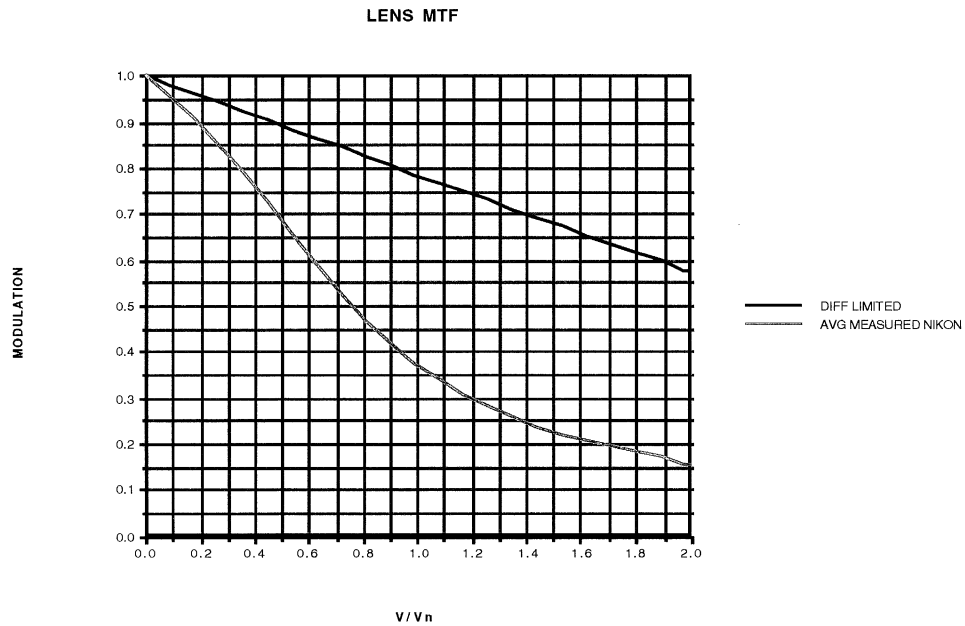
**Figure 17: 28 mm Nikon Lens Transmittance Plot**

The lens fall-off (fall-off of intensity as a function of field angle) was also measured and incorporated into the model by using a average  $\text{COS}^3$  and  $\text{COS}^4$  function (see Figure 18). This roll-off factor is important in comparing on-axis data to off-axis data. Since the 460 camera has a significantly larger field than the 420 version, the lens roll-off will have a much larger impact in final performance. As shown below in Figure 18, the 460 camera's energy falls off substantially out in the field. The model uses a LUT for lens roll-off prediction. Currently, the model assumes a lens focal length of 28 mm and is capable of predicting on-axis, half-field, and full-field point radiometric performance.



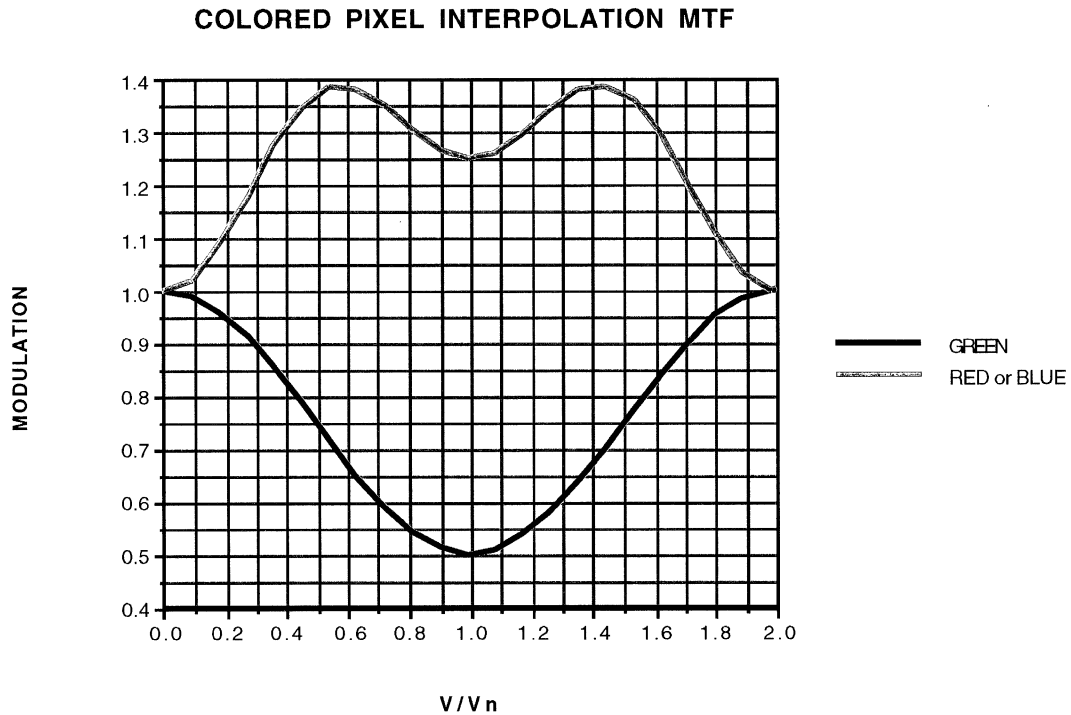
**Figure 18: 28 mm Lens Fall-Off Plot**

Figure 19 shows the Lens MTF of the Nikon 28 mm lens. The Nikon lens was measured with the 650BP300 band-pass filter screwed onto it. This data was taken at half-field in the radial direction. The focus position was kept at the on-axis best focus point. The top curve is the F/5.6 diffraction limited lens<sup>14</sup>. Notice that the Nikon lens is far from being diffraction limited. This lens is typical for off-the-shelf consumer lenses.



**Figure 19: Lens MTF Plot**

Figure 20 shows the driver interpolation MTF for the three color pixels. The interpolation MTF is a result of the Bayer pattern architecture<sup>1</sup>. The interpolation MTF is scene dependent and is therefore modeled as a weighted average MTF. The red pixel and blue pixel MTFs are identical. Note, the red and blue pixels are intrinsically influenced by the green pixel. The resulting MTF curves are clearly color distinct. Because of this MTF color distinction, some images will suffer from color aliasing of some objects. The presence of color aliasing can be seen in Table 4 of the Results section of this paper .



**Figure 20: Color Interpolation MTF Plot**

### 3.2.4 Radiometric Model Equations

The following two sub-sections (3.2.4 and 3.2.5) rigorously define and detail the equations used in the model. Sub-section 3.2.4 concentrates on the equations used in the radiometric portion of the model. The main reference sources for these equations are: Schott<sup>13</sup>, Dereniak and Crowe<sup>4</sup>, Boyd<sup>2</sup>, and Ekiert<sup>9</sup>. These equations analytically describe the radiometric attributes of the entire imaging chain (from the sun's radiation to the target's reflectance to the camera's digital count output).

**Total spectral solar radiance reaching the front of the sensor<sup>13</sup>:  $L_{\text{sensor-frt}}$**   
**[watts / (meter<sup>2</sup> \* micron \* steradian)]**

$$L_{\text{sensor-frt}}(\lambda) = E'_s(\lambda) * \tau_1(\lambda) * \cos(\sigma) * (r(\lambda)/\pi) * \tau_2(\lambda) + \tau_2(\lambda) * r(\lambda) * L_d(\lambda) + L_u(\lambda) \quad (\text{R1})$$

where:

$E'_s(\lambda)$  is the exoatmospheric irradiance [watts / (meter<sup>2</sup> \* micron)]

$\tau_1(\lambda)$  is the atmospheric spectral transmittance along the sun to target path [%]

$\sigma$  is the solar zenith angle [degrees]

$r(\lambda)$  is the target spectral reflectance [%]

$\tau_2(\lambda)$  is the atmospheric spectral transmittance along the target to sensor path [%]

$L_d(\lambda)$  is the downwelled solar radiance [watts / (meter<sup>2</sup> \* micron \* steradian)]

$L_u(\lambda)$  is the path solar radiance [watts / (meter<sup>2</sup> \* micron \* steradian)]

-or - the total spectral solar radiance reaching the front of the sensor can be expressed in terms of its signal and haze components:

$$L_{\text{sensor-frt}}(\lambda) = L_{\text{sensor-frt,signal}}(\lambda) + L_{\text{sensor-frt,haze}}(\lambda) \quad (\text{R2})$$

where:

$$L_{\text{sensor-frt,signal}}(\lambda) = E'_s(\lambda) * \tau_1(\lambda) * \cos(\sigma) * (r(\lambda)/\pi) * \tau_2(\lambda) + \tau_2(\lambda) * r(\lambda) * L_d(\lambda)$$

$$L_{\text{sensor-frt,haze}}(\lambda) = L_u(\lambda)$$

**Total irradiance at the detector (or pixel)<sup>2,4,13</sup>;  $E_{\text{e,det}}(\lambda)$**   
**[watts / (meter<sup>2</sup> \* micron)]**

$$E_{\text{e,det}}(\lambda) = \pi * L_{\text{sensor-frt}}(\lambda) * T_{\text{bpf}}(\lambda) * T_{\text{lens}}(\lambda) / ((4 * F/\#^2) + 1) \quad (\text{R3})$$

where:

$L_{\text{sensor-frt}}(\lambda)$  is the total spectral radiance reaching the front of the sensor

$T_{\text{bpf}}$  is the spectral transmittance of the band-pass filter in front of the lens [%]

$T_{\text{lens}}$  is the spectral transmittance of the lens [%]

$F/\#$  is F number of the lens = focal length / entrance pupil diameter



- or - the total irradiance at the detector (or pixel); can be expressed in terms of its signal and haze components:

$$E_{e,det}(\lambda) = E_{e,det,signal}(\lambda) + E_{e,det,haze}(\lambda) \quad (R4)$$

where:

$$E_{e,det,signal}(\lambda) = \pi * L_{sensor-frt,signal}(\lambda) * T_{bpf}(\lambda) * T_{lens}(\lambda) / ((4 * F/\#^2) + 1)$$

$$E_{e,det,haze}(\lambda) = \pi * L_{sensor-frt,haze}(\lambda) * T_{bpf}(\lambda) * T_{lens}(\lambda) / ((4 * F/\#^2) + 1)$$

**Total irradiance at the detector (or pixel)<sup>4</sup>;  $E_{p,det}(\lambda)$   
[photons / (meter<sup>2</sup> \* micron \* second)]**

$$E_{p,det}(\lambda) = E_{e,det}(\lambda) * \lambda / (h * c) \quad (R5)$$

where:

$\lambda$  = emitted photon wavelength [microns]

$h$  = Planck's constant ( $6.6262 \times 10^{-34}$  Wsec<sup>2</sup>)

$c$  = speed of light ( $2.999 \times 10^8$  m/sec)

-or-

$$E_{p,det}(\lambda) = E_{p,det,signal} + E_{p,det,haze} \quad (R6)$$

where:

$$E_{p,det,signal}(\lambda) = E_{e,det,signal}(\lambda) * \lambda / (h * c)$$

$$E_{p,det,haze}(\lambda) = E_{e,det,haze}(\lambda) * \lambda / (h * c)$$

**Total electrons due to solar radiation for a given wavelength;  $e_{num}$   
[electrons]**

$$e_{num}(\lambda) = E_{p,det}(\lambda) * \eta(\lambda) * A_{det} \quad (R7)$$

where:

$E_{p,det}(\lambda)$  [photons / (meter<sup>2</sup> \* micron \* second)]

$\eta(\lambda)$  is the quantum efficiency of the detector [%]

$A_{det}$  is the area of the detector or pixel [meter<sup>2</sup>]

-or-

$$e_{\text{num}}(\lambda) = e_{\text{num,signal}}(\lambda) + e_{\text{num,haze}}(\lambda) \quad (\text{R8})$$

where:

$$e_{\text{num,signal}}(\lambda) = E_{\text{p,det,signal}}(\lambda) * \eta(\lambda) * A_{\text{det}}$$

$$e_{\text{num,haze}}(\lambda) = E_{\text{p,det,haze}}(\lambda) * \eta(\lambda) * A_{\text{det}}$$

**Total electrons due to solar radiation for a given wavelength band;  $e_{\text{num,wb}}$  [electrons]**

$$e_{\text{num,wb}}(\lambda) = e_{\text{num}}(\lambda) * \Delta_{\lambda} \quad (\text{R9})$$

where:

$e_{\text{num}}(\lambda)$  is the number of electrons for a given wavelength

$\Delta_{\lambda}$  is the wavelength bandwidth [microns]

-or-

$$e_{\text{num,wb}}(\lambda) = e_{\text{num,wb,signal}}(\lambda) + e_{\text{num,wb,haze}}(\lambda) \quad (\text{R10})$$

where:

$$e_{\text{num,wb,signal}}(\lambda) = e_{\text{num,signal}}(\lambda) * \Delta_{\lambda}$$

$$e_{\text{num,wb,haze}}(\lambda) = e_{\text{num,haze}}(\lambda) * \Delta_{\lambda}$$

**Total number of electrons at the detector or pixel due to solar radiation;  $e_{\text{det}}$  [electrons]**

$$e_{\text{det}} = \sum e_{\text{num,wb}}(\lambda) ; \text{summed over the defined wavelength band} \quad (\text{R11})$$

-or-

$$e_{\text{det}} = \sum ( e_{\text{num,wb,signal}}(\lambda) + e_{\text{num,wb,haze}}(\lambda) ) \quad (\text{R12})$$

**Total number of electrons for a monochrome pixel;  $e_{\text{det,m}}$  [electrons]**

$$e_{\text{det,m}} = e_{\text{det}} \quad \text{-or-} \quad (\text{R13})$$

$$e_{\text{det,m}} = e_{\text{det,m,signal}} + e_{\text{det,m,haze}} \quad (\text{R14})$$

**Total number of electrons for a red pixel due to solar radiation;  $e_{det,r}$  [electrons]**

$$e_{det,r} = \sum ( T_{cfa,r}(\lambda) * e_{num,wb}(\lambda) ) ; \text{summed over the defined wavelength band} \quad (R15)$$

where:

$T_{cfa,r}(\lambda)$  is the color filter array red pixel spectral transmittance [%]

-or-

$$e_{det,r} = e_{det,r,signal} + e_{det,r,haze} \quad (R16)$$

where:

$$e_{det,r,signal} = \sum ( T_{cfa,r}(\lambda) * e_{num,wb,signal}(\lambda) )$$

$$e_{det,r,haze} = \sum ( T_{cfa,r}(\lambda) * e_{num,wb,haze}(\lambda) )$$

likewise, the total number of electrons for the green and blue pixels due to solar radiation is computed in a similar manner.

**Total RMS number of electrons due to sensor and electronic noise<sup>9,13</sup>;  $e_{s\&enoi se}$  [electrons]**

$$e_{s\&enoi se} = \sqrt{ (e_{sensornoise})^2 + (e_{shotnoise})^2 + (e_{quannoise})^2 } \quad (R17)$$

where:

$e_{sensornoise}$  = sensor noise

$e_{shotnoise}$  = shot noise =  $\sqrt{e_{det}}$

$e_{quannoise}$  = quantization noise =  $e_{det} / (2^{\#bit} * \sqrt{12})$

where:

#bit = the number of bits (8 or 12)

**Grand total number of electrons;  $e_{sum}$  [electrons]**

$$e_{sum} = e_{det} + e_{s\&enoi se} \quad (R18)$$

**Camera Digital Counts:**

$$\text{8-bit counts for SIGNAL e's} = \text{ROUND} (e_{\text{det,signal}} / \Gamma) \quad (\text{R19})$$

$$\text{8-bit counts for HAZE e's} = \text{ROUND} (e_{\text{det,b,haze}} / \Gamma) \quad (\text{R20})$$

$$\text{8-bit counts for total (sig + haze) e's} = \text{ROUND} (e_{\text{det,b}} / \Gamma) \quad (\text{R21})$$

$$\begin{aligned} \text{8-bit counts for total sensor and electronics noise e's} \\ = \text{ROUND} (e_{\text{s\&enose}} / \Gamma) \end{aligned} \quad (\text{R22})$$

$$\text{8bit counts for grand total e's} = \text{ROUND} (e_{\text{sum}} / \Gamma) \quad (\text{R23})$$

where:

$$\Gamma = \text{quantization interval} = (\partial / 2^{\#\text{bit}})$$

where:  $\partial$  = detector saturation level in electrons

The 12-bit digital count equations are identical to the 8-bit equations, except the #bits = 12 instead of 8.

### 3.2.5 Image Quality Model Equations

Sub-section 3.2.5 outlines the equations for the image quality portion of the model. The main reference sources for these equations are: Ekiert<sup>9</sup>, Schott<sup>13</sup>, and Tantalo<sup>15</sup>. These equations analytically define all of the imaging chain component's contributions to the final image quality of the output image. By using a linear system approach (i.e. TMA), the model cascades all of the appropriate contributions to predict a final camera resolution.

**Ground sample distance:  $GSD_{it}^{9,13}$ ;  $GSD_{ct}$**

$$GSD_{it} = (P_{it} * A) / FL \quad (IQ1A)$$

$$GSD_{ct} = (P_{ct} * A) / FL \quad (IQ1B)$$

where;

$P_{it}$  = in-track pixel size

$P_{ct}$  = cross-track pixel size

A = aircraft altitude above the ground

FL = focal length of the lens

**Nyquist limited ground resolving distance<sup>9,13</sup>:  $GRD_{nyqt}$**

$$GRD_{nyqt,it} = 2 * GSD_{it} \quad (IQ2A)$$

$$GRD_{nyqt,ct} = 2 * GSD_{ct} \quad (IQ2B)$$

#### MTFs

$\nu$  denotes the frequency for the in-track spatial direction

$\eta$  denotes the frequency for the cross-track spatial direction

**Atmospheric MTF:  $MTF_{atmos}(\nu)$ ;  $MTF_{atmos}(\eta)$**

$$MTF_{atmos}(\nu) = MTF_{atmos}(\eta) = \text{constant for all frequencies} \quad (IQ3)$$

**Aircraft linear motion MTF:  $MTF_{aircraft}(\nu)^{9,13}$ ;  $MTF_{aircraft}(\eta)$**

$$MTF_{aircraft}(\nu) = \text{sinc}(\nu * \nabla_{eqamt} * P_{it}) \quad (IQ4A)$$

where:

$\nabla_{eqamt}$  = equivalent pixel factor =  $\Omega / P_{it}$

$\Omega_{it}$  = in-track smear amount = aircraft speed<sub>it</sub> \* integration time \* (fl / ALT)

$P_{it}$  = pixel size in the in-track direction

$$MTF_{aircraft}(\eta) = \text{sinc}(\eta * \nabla_{eqamt} * P_{ct}) \quad (IQ4B)$$

where:

$\nabla_{eqamt}$  = equivalent pixel factor =  $\Omega / P_{ct}$

$\Omega_{ct}$  = cross-track smear amount = aircraft speed<sub>ct</sub> \* integration time \* (fl / ALT)  
 $P_{ct}$  = Pixel size in the cross-track direction

The following three figures, show the effects of integration time, aircraft speed, and altitude on the  $MTF_{aircraft}$ .

**AIRCRAFT MOTION MTF (LINEAR SMEAR)**

**FL= 28 MM; PIXEL = 9 MIC; ALT. = 3000 FT; SPEED = 100 MPH**

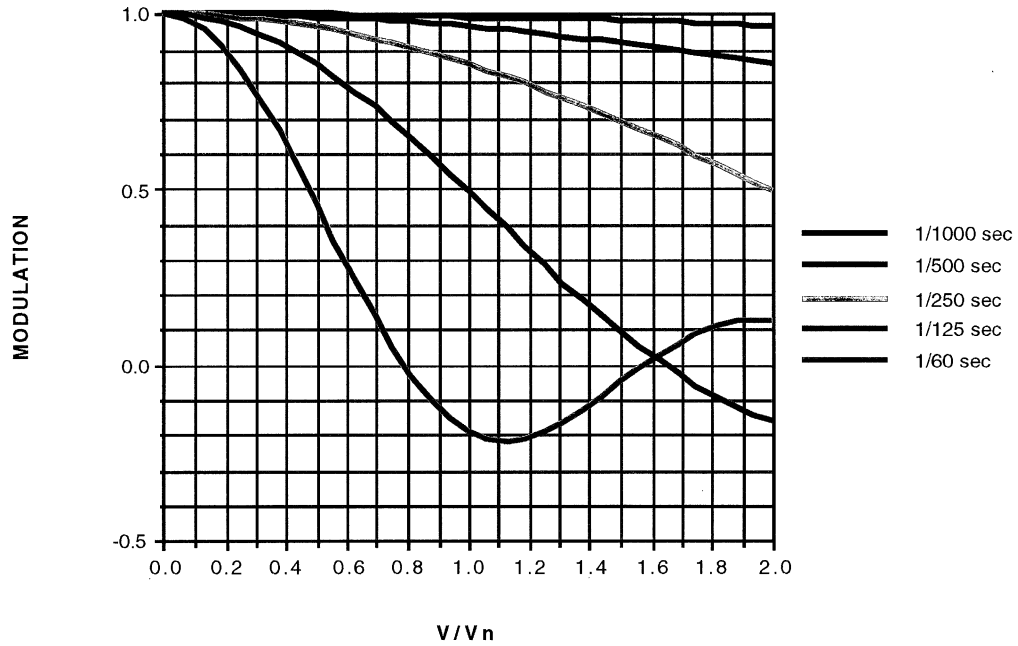


**Figure 21: Aircraft Motion MTF for Various Integration Times Plot**

**AIRCRAFT MOTION MTF (LINEAR SMEAR)**

**FL = 28 MM; PIXEL = 9 MIC; ALT = 3000 FT; SHUTTER = 1/250 SEC**

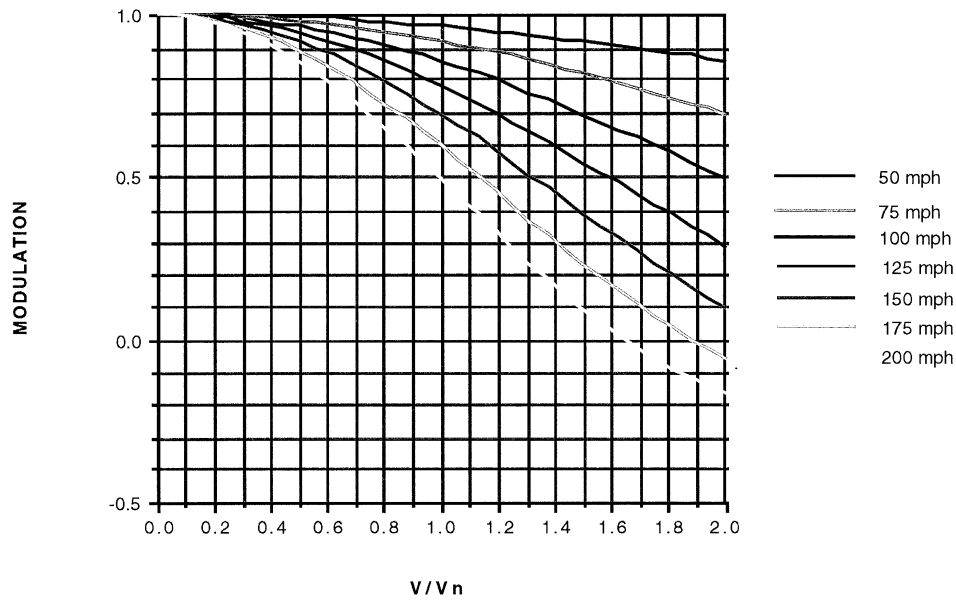


**Figure 22: Aircraft Motion MTF for Various Aircraft Speeds Plot**

**AIRCRAFT MOTION MTF (LINEAR SMEAR)**

**FL = 28 MM; PIXEL = 9 MIC; SPEED = 100 MPH ; SHUTTER = 1/250 SEC**

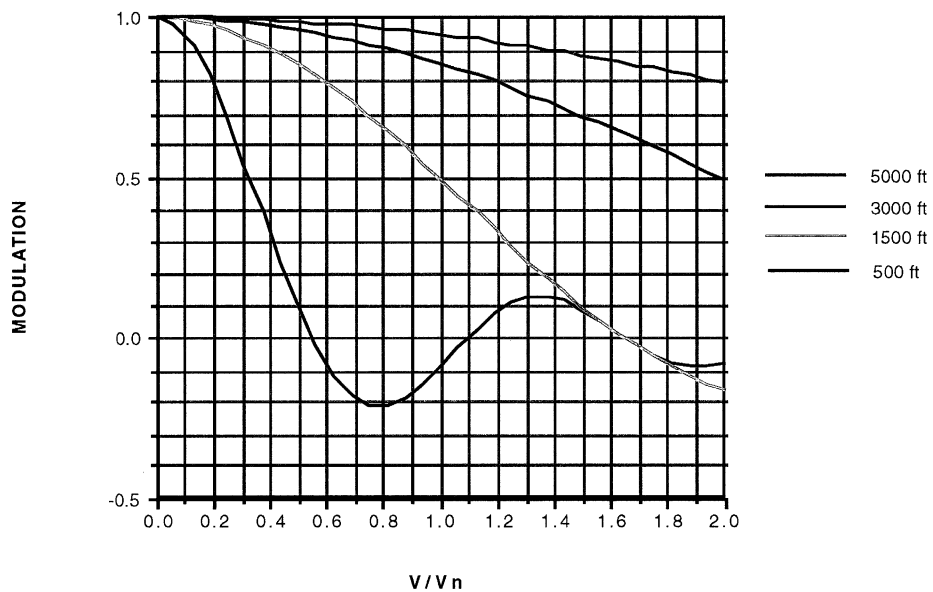


**Figure 23: Aircraft Motion MTF for Various Aircraft Altitudes Plot**

**Optics MTF: Diffraction limited circular aperture lens MTF<sup>14</sup>: MTF(v)<sub>diff lens</sub>**

$$MTF(v)_{diff lens} = (2/\pi) * (\phi - \cos(\phi) * \sin(\phi)) * \cos(\theta)^k = MTF(\eta)_{diff lens} \quad (IQ5)$$

where:

$$\phi = \cos^{-1}(v/v_o)$$

$$v_o = 1/(\lambda * F/\#)$$

$\theta$  = is the half angle

$k = 1$  for radial lines and 3 for tangential lines

**Detector MTF: MTF<sub>det</sub>(v)<sup>9,13,15</sup>; MTF<sub>det</sub>( $\eta$ )**

$$MTF_{det}(v) = \text{sinc}(v * P_{it}) \quad (IQ6A)$$

where  $P_{it}$  = pixel size in the in-track direction

$$MTF_{det}(\eta) = \text{sinc}(\eta * P_{ct}) \quad (IQ6B)$$

where:  $P_{ct}$  = pixel size in the cross-track direction

**Charge transfer MTF: MTF<sub>chg</sub>(v)<sup>9</sup>; MTF<sub>chg</sub>( $\eta$ )**

$$MTF_{chg}(v) = \text{EXP}[-\gamma_{it} (1-\epsilon)(1-\cos(\alpha_{it}))] \quad (IQ7A)$$

where:  $\gamma_{it}$  = # of charge transfers in the in-track direction

$\epsilon$  = charge transfer efficiency

$$\alpha_{it} = 2 * \pi * P_{it} * v$$

$$MTF_{chg}(\eta) = \text{EXP}[-\gamma_{ct} (1-\epsilon)(1-\cos(\alpha_{ct}))] \quad (IQ7B)$$

where:  $\gamma_{ct}$  = # of charge transfers in the in-track direction

$\epsilon$  = charge transfer efficiency

$$\alpha_{ct} = 2 * \pi * P_{ct} * \eta$$

**Detector clocking MTF: MTF<sub>clock</sub>(v)<sup>9</sup>; MTF<sub>clock</sub>( $\eta$ )**

$$MTF_{clock}(v) = \text{sinc}(v * P_{it} / \Phi_{clock}) \quad (IQ8A)$$

$$MTF_{clock}(\eta) = \text{sinc}(\eta * P_{ct} / \Phi_{clock}) \quad (IQ8B)$$

where:  $\Phi_{clock}$  = # of phase clocks



**Interpolation MTF (weighted average MTF)<sup>1</sup>:**

**Green interpolation:  $MTF_{\text{interp,grn}}(v)$ ;  $MTF_{\text{interp,grn}}(\eta)$**

$$MTF_{\text{interp,grn}}(v) = 0.75 + (0.25 * \text{COS}(2 * \pi * v / (2 * v_n))) \quad (\text{IQ9A})$$

$$MTF_{\text{interp,grn}}(\eta) = 0.75 + (0.25 * \text{COS}(2 * \pi * \eta / (2 * \eta_n))) \quad (\text{IQ9B})$$

where:

$$v_n = \text{Nyquist frequency} = 1 / (2 * P_{it})$$

$$\eta_n = \text{Nyquist frequency} = 1 / (2 * P_{ct})$$

**Red interpolation:  $MTF_{\text{interp,red}}(v)$ ;  $MTF_{\text{interp,red}}(\eta)$**

$$MTF_{\text{interp,red}}(v) = MTF_{\text{interp,grn}}(v) + (0.5 + (2 * (-0.1875) * \text{COS}(2 * \pi * v / (2 * v_n))) + (2 * (-0.0625) * \text{COS}(4 * \pi * v / (2 * v_n)))) \quad (\text{IQ10A})$$

$$MTF_{\text{interp,red}}(\eta) = MTF_{\text{interp,grn}}(\eta) + (0.5 + (2 * (-0.1875) * \text{COS}(2 * \pi * \eta / (2 * \eta_n))) + (2 * (-0.0625) * \text{COS}(4 * \pi * \eta / (2 * \eta_n)))) \quad (\text{IQ10B})$$

**Blue interpolation:  $MTF_{\text{interp,blue}}(v)$ ;  $MTF_{\text{interp,blue}}(\eta)$**

$$MTF_{\text{interp,blue}}(v) = MTF_{\text{interp,red}}(v) \quad (\text{IQ11A})$$

$$MTF_{\text{interp,blue}}(\eta) = MTF_{\text{interp,red}}(\eta) \quad (\text{IQ11B})$$

## Threshold Modulation Analysis<sup>9</sup>

### Input modulation: ITM

$$ITM = MTF_{atmos} * MTF_{aircraft} * MTF_{optics} * MOD_{target} \quad (IQ12)$$

where:

$$MOD_{target} = \text{target modulation} = (C-1) / (C+1) \quad (IQ13)$$

$$C = \text{target to background contrast} = NDVI_{target} / NDVI_{background} \quad (IQ14)$$

### Required modulation: TM

$$TM = (\sqrt{(SNR_{req} * MOD_{noise})^2 + TM_{vis}}) / (MTF_{det} * MTF_{chg} * MTF_{clock} * MTF_{elec} * MTF_{interp}) \quad (IQ15)$$

where:

$SNR_{req}$  = required minimum SNR for the eye

$$MOD_{noise} = \text{noise modulation} = e_{s\&noise} / e_{det,sig} \quad (IQ16)$$

where:

$e_{s\&noise}$  = total RMS number of electrons due to sensor & electronic noise

$e_{det,sig}$  = total number of electrons due to signal

$TM_{vis}$  = required minimum modulation for the eye

## 4.0 Results

### 4.1 Flight Test Data

Figure 21 shows the results of flight test raw image going through two different Photoshop drivers. The flight test image (see Appendix 1) is the large Macbeth target @  $\approx 1300$  feet AGL with the 28 mm lens. The X-axis is the average reflectance of the neutral gray patches. The CIR v3.0.1 with gamma = 1.0 driver and a linear driver. The CIR driver is a standard CIR driver that comes with the camera. The linear driver is a driver that can be obtained by special request. Note the linear driver does not backout the infrared signal from the red and green pixels channels.

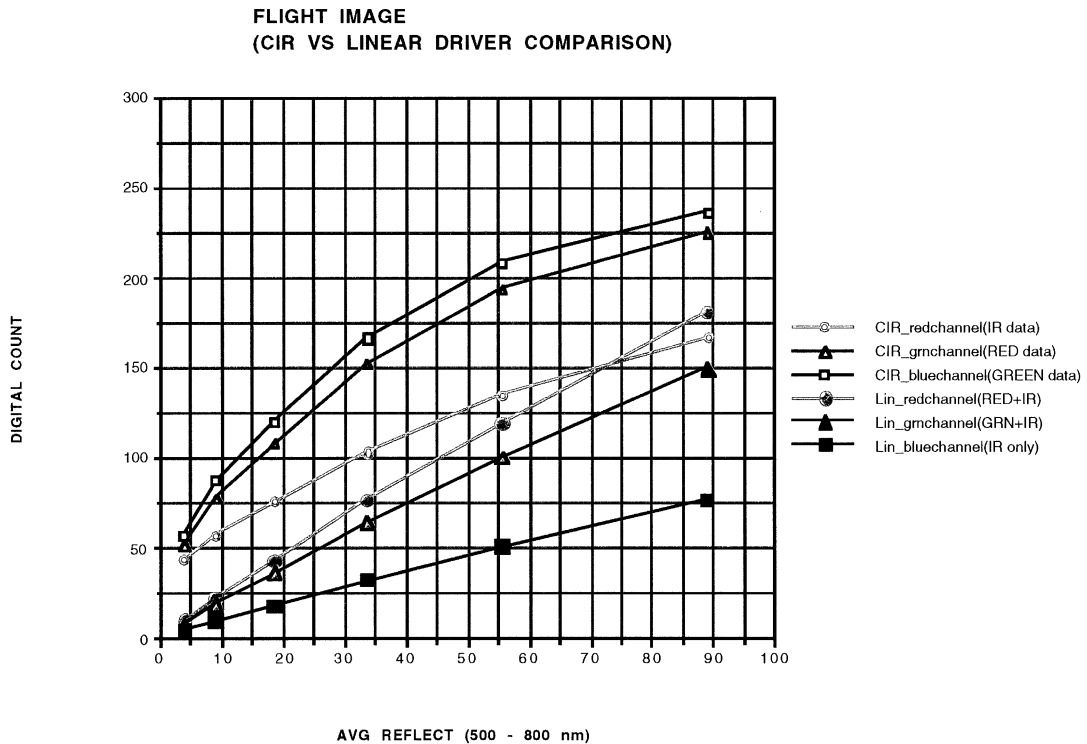


**Figure 24: Driver Comparison Plot**

## 4.2 Modeling Case Study - Three Wheat Curves

A modeling case study of wheat changes throughout the growing season was performed. The case study was used to show the utility of a CIR camera and the analytical model. The study compared the three temporal wheat curves shown previously in Figure 16. The study had the following input parameters:

Camera: 460 CIR  
 Filter: 650BP300  
 Lens: 28 mm  
 F/#: F/5.6  
 Integration Time: 0.002, 0.004, 0.0067, 0.008, 0.01667 sec.  
 Altitude: 3000 feet  
 Aircraft Speed: 50, 100, 150, 200, 250, 300, 350 mph  
 Target: Wheat data (Figure 16)  
 Atmosphere: Roch-23, Roch-7, Roch-5+  
 Field of View: On-axis; Half-Field, Full-Field  
 Solar Angle: 30 degree

The results of the study are shown in the following four tables. The first three tables are radiometric summaries while the fourth table is an image quality summary for the study. Table 1 summarizes the camera response differences from the different wheat inputs.

***** WHEAT DIFFERENTIATION *****											
CAMERA -> 460											
ATMOS -> ROCH-23											
FILTER -> 650BP											
F/# -> F/5.6											
TARGET -> WHEAT-GRN											
SUN ZEN -> 30											
	REL.		MATRIX RED (RED)		MATRIX GRN (GREEN)		MATRIX BLUE (IR)		NDVI		
	FLD	expos.	tot'l	sig'l	tot'l	sig'l	tot'l	sig'l	tot'l	sig'l	
	0.0	0.002	22	8	23	4	74	64	0.542	0.778	
	0.0	0.004	44	16	46	8	148	128	0.542	0.778	
	<b>0.0</b>	<b>0.0067</b>	<b>73</b>	<b>27</b>	<b>77</b>	<b>13</b>	<b>246</b>	<b>213</b>	<b>0.542</b>	<b>0.775</b>	
	0.0	0.008	88	32	92	16	296	256	0.542	0.778	
	0.0	0.01667	183	66	191	34	615	533	0.541	0.780	
CAMERA -> 460											
ATMOS -> ROCH-23											
FILTER -> 650BP											
F/# -> F/5.6											
TARGET -> WHEAT-NEW											
SUN ZEN -> 30											
	REL.		MATRIX RED (RED)		MATRIX GRN (GREEN)		MATRIX BLUE (IR)		NDVI		
	FLD	expos.	tot'l	sig'l	tot'l	sig'l	tot'l	sig'l	tot'l	sig'l	
	<b>0.0</b>	<b>0.0067</b>	<b>108</b>	<b>62</b>	<b>89</b>	<b>25</b>	<b>180</b>	<b>147</b>	<b>0.250</b>	<b>0.407</b>	
	0.0	0.008	130	74	106	31	216	177	0.249	0.410	
	0.0	0.01667	271	154	221	64	450	369	0.248	0.411	
CAMERA -> 460											
ATMOS -> ROCH-23											
FILTER -> 650BP											
F/# -> F/5.6											
TARGET -> WHEAT-NORM											
SUN ZEN -> 30											
	REL.		MATRIX RED (RED)		MATRIX GRE (GREEN)		MATRIX BLUE (IR)		NDVI		
	FLD	expos.	tot'l	sig'l	tot'l	sig'l	tot'l	sig'l	tot'l	sig'l	
	<b>0.0</b>	<b>0.0067</b>	<b>66</b>	<b>20</b>	<b>88</b>	<b>24</b>	<b>201</b>	<b>168</b>	<b>0.506</b>	<b>0.787</b>	
	0.0	0.008	79	24	105	29	241	202	0.506	0.788	
	0.0	0.01667	165	49	219	61	503	421	0.506	0.791	

Table 1: Wheat Differentiation



Table 3 shows the effects of different atmospheres on the imaging process. Atmospheres Roch-7 and Roch-5+ give some spurious results. This indicates that the two atmospheres are too water saturated for good imaging results.

***** ATMOSPHERIC EFFECT *****											
CAMERA -> 460											
FLD PT -> 0.0											
FILTER -> 650BP											
F/# -> F/5.6											
TARGET -> WHEAT-GRN											
SUN ZEN -> 30											
	ATMOS	expos.		MATRIX RED (RED)		MATRIX GRN (GREEN)		MATRIX BLUE (IR)		NDVI	
			tot'l	sig'l	tot'l	sig'l	tot'l	sig'l	tot'l	sig'l	
	roch-23	0.01667	183	66	191	34	615	533	0.541	0.780	
	roch-7	0.01667	136	1	160	0	109	10	-0.110	0.810	
	roch-5+	0.01667	265	2	320	0	252	66	-0.025	0.941	
CAMERA -> 460											
FLD PT -> 0.0											
FILTER -> 650BP											
F/# -> F/5.6											
TARGET -> WHEAT-NEW											
SUN ZEN -> 30											
	ATMOS	expos.		MATRIX RED (RED)		MATRIX GRN (GREEN)		MATRIX BLUE (IR)		NDVI	
			tot'l	sig'l	tot'l	sig'l	tot'l	sig'l	tot'l	sig'l	
	roch-23	0.01667	271	154	221	64	450	369	0.248	0.411	
	roch-7	0.01667	137	2	160	1	106	6	-0.128	0.5	
	roch-5+	0.01667	276	13	323	3	231	44	-0.089	0.544	
CAMERA -> 460											
FLD PT -> 0.0											
FILTER -> 650BP											
F/# -> F/5.6											
TARGET -> WHEAT-NORM											
SUN ZEN -> 30											
	ATMOS	expos.		MATRIX RED (RED)		MATRIX GRN (GREEN)		MATRIX BLUE (IR)		NDVI	
			tot'l	sig'l	tot'l	sig'l	tot'l	sig'l	tot'l	sig'l	
	roch-23	0.01667	165	49	219	61	503	421	0.506	0.791	
	roch-7	0.01667	135	1	160	1	107	8	-0.116	0.778	
	roch-5+	0.01667	264	1	323	2	239	52	-0.05	0.962	

**Table 3: Atmospheric Impact on NDVI Predictions**

Table 4 shows results of the image quality analysis. Note, the NDVI calculated in the radiometric analysis was used to compute the target contrast. The table clearly shows the WHEAT-GRN can easily be distinguished from the WHEAT-NEW. The WHEAT-GRN and the WHEAT-NORM are too similar to easily detect the difference. Note that for various aircraft speed, various components of the imaging change dominate the results. Also, note the presence of color aliasing as seen from the differences in GRD between the green and blue channels.

<b>*****FROM RADIOMETRIC MODEL*****</b>							
ALT=	3000FT			NDVI	CONTRAST	MOD	
F/# =	F/5.6			(IR-RED)/(IR+RED)	NDVI1/NDVI2	(C-1)/(C+1)	
FL=	28mm	<b>TARGET</b>					
PIXEL=	9MICRON	WHEAT-GRN		0.775	na		
ATMOS=	ROCH-23	WHEAT-NEW		0.407		1.904	0.311
SHUTTER =	1/150	WHEAT-NORM		0.787		1.015	0.008
TARGET e- =	48,100						
HAZE e- =	26,500						
GSD(in)=	11.57						
NYQUIST GRD(in)=	23.14						
<b>WHEAT-NEW TO WHEAT-GREEN COMPARISON</b>							
<b>***** PREDICTED GRD(in)*****</b>							
AIRCRAFT SPEED->	<b>50.0</b>	<b>100.0</b>	<b>150.0</b>	<b>200.0</b>	<b>250.0</b>	<b>300.0</b>	<b>350.0</b>
PIXEL SMEAR->	0.51	1.010	1.52	2.03	2.53	3.04	3.55
<b>LENS PIXEL</b>							
IFF LIMITED GREEN	23.14	23.14	24.39	25.71	27.27	29.16	31.49
BLUE	23.14	23.14	23.14	24.39	27.27	29.16	31.49
AVG. MEASURED LENS							
GREEN	23.26	24.39	25.71	27.27	29.16	31.49	31.49
BLUE	23.14	23.14	23.26	25.71	27.27	29.16	31.49
<b>WHEAT-NORM TO WHEAT-GREEN COMPARISON</b>							
<b>***** PREDICTED GRD(in)*****</b>							
GRD = 257.14in							
-> NOT ENOUGH CONTRAST TO DETECT A DIFFERENCE							
Q: WHAT IS THE MINIMUM ALLOABLE TARGET CONTRAST WHICH CAN BE DETECTED?							
ALT=	3000FT						
F/#=	F/5.6						
FL=	28mm						
PIXEL=	9MICRON						
ATMOS=	ROCH-23						
SHUTTER=	1/150						
SPEED=	100mph						
LENS=	AVG. MEASURED						
<b>A: THE MINIMUM ALLOWABLE CONTRAST TO DETECT CHANGE IS 1.0661</b>							
<b>-&gt;NDVI = 0.8262 ( ASSUMING WHEAT-GRN AS THE REF)</b>							
	PIXEL	GRD(in)					
	GREEN	257.14					
	BLUE	181.83					

**Table 4: Wheat Case-Study Image Quality Summary**

## 5.0 Conclusion / Summary

The project has been very helpful on understanding the technical aspects of the CIR camera and its usefulness for remote sensing. The project's main focus of creating an analytical model of the CIR camera has been successfully accomplished. Clearly, the model can be useful to predict both radiometric and image quality camera performance in airborne applications. From the results presented, it is clear that the camera has excellent image capture capabilities for remote sensing applications. Because of the camera's unique filtering flexibility, one can only imagine the imaging possibilities. With the use of the model, one can easily predict and optimize performance before costly aerial flights occur. As presented throughout this paper, the measured data will be very useful for future analysis on other imaging research projects.

*Suggestion for Future Follow-on Work*

### **Lab and Field Radiometric Camera Calibration Testing**

A better understanding of the actual camera output relative to the model's results needs to be explored. One approach, to baseline the camera's actual performance, involves the use of an integrating sphere and a calibrated blackbody light source. The light source could be easily filtered and therefore, camera output to known spectral radiance input data could be collect. The results of this valuable lab data could be incorporated into the model to incorporate the offsets and gain parameters in the color balance section of the model. Once the lab work was completed, a similar experiment could be performed outside using multiple cameras at multiple altitudes to better understand the atmospheric impacts on the camera performance.

### **Modeling the Current Driver V3.0.3 Interpolation**

The model currently does not perform the color interpolation function that the camera software driver does. Currently, the color interpolation technique used in the driver is a Kodak proprietary algorithm. If the proprietary algorithm was incorporated into the model, it would enhance its accuracy and predictability. One could also compare the results of the data with results from using another interpolation to see if there is a better choice for interpolations when radiometric integrity of the data is essential.



### **Filter Study**

The model could be used to design and optimize new band-pass filters based on unique detection applications. The current band-pass filter was designed for pest detection in forests. While this filter works well for other applications, it probably is not the optimal filter for every remote sensing application. Broader band passes and/or narrower band passes may yield better results for certain applications.

### **Measured Temporal Spectral Reflectance Data of Various Plants**

Currently, the model only has wheat incorporated for temporal studies. One could easily incorporate other types of crop data into the model once the data is measured or is located. Note the model used spectral reflectance data from 400 nm to 1000 nm at 5 nm increments.

### **8-bit vs 12-bit vs 14-bit**

The model predicts both 8-bit and 12-bit radiometric results. One could perform a study to predict the enhanced detection capabilities of the camera if 12-bit or even 14-bit data was accessible to the end user. Currently, the CIR camera does not let the end user have access to the original 12-bit. If the results of a larger dynamic range study show significant improvements for remote sensing, there may be ways to incorporate this into the camera. The modifications needed to the camera must be compared to the cost of implementing these changes to see if it is financially beneficial.

### **Visual Simulations**

Incorporation of the CIR camera parameters into DIRSIG. This would help further validate the camera model. Also, once the camera parameters are in DIRSIG, visual simulations of the CIR camera 's output image can easily be generated. One interesting visual simulation that could be produced, is the color aliasing artifacts caused by under sampling a busy scene and the color interpolation processing<sup>15</sup>.

## 6.0 Appendix

**Appendix 1 - Flight Test Image**



**Appendix 2 - NDVI Image of the Flight Test Image**



### **Appendix 3 - Radiometric Model Sample Run**

CONSTANTS:	FOURBLACKBODY EMITTER	INPUTS:	FIELD POINT	LENS FALL-OFF ENERGY FACTOR	SIGNAL ONLY Radiance at Detector (Watts/m <sup>2</sup> um <sup>2</sup> sr)
M = SPECTRAL RADIANT EXITANCE (g/sec cm <sup>2</sup> um)	460	CAMERA TYPE(420 or 460)=	0.000	420	68.999
E = SPECTRAL IRRADIANCE AT THE DETECTOR (g/sec cm <sup>2</sup> um)	0	FIELD POINT(0.0,0.0,0.25,0.0,0.75,1.0)=	0.000	460	73.530
WL = EMITTED WAVELENGTH IN (UM)	400	PIXEL SIZE (um) =	0.000	420	77.014
T = BLACKBODY TEMP IN (DEG K)	405	FILL FACTOR =	0.250	460	79.418
c = SPEED OF LIGHT	410	SATURATION LEVEL(%) =	0.500	420	81.262
k = BOLTZMANN'S CONSTANT	415	SENSOR NOISE (e-)=	0.750	460	82.669
h = PLANCK'S CONSTANT	420	FL(mm) =	1.000	420	83.780
h = PLANCK'S CONSTANT	425	F/# =	0.005	460	84.666
h = PLANCK'S CONSTANT	430	T(sec) =	0.09	420	85.417
Rs = SUN RADIUS	435	SUN ZENITH ANG(deg)=	30.00	460	86.674
Res = EARTH TO SUN DISTANCE	440	OPTIONS FOR TARGET REFLECT	1	420	87.720
	445	White		460	88.245
	450	Neutral-5		420	88.689
	455	Neutral-3.5		460	89.064
	460	Black		420	89.375
	465	WHEAT-GRN		460	89.820
	470	WHEAT-NEW		420	90.103
	475	WHEAT-NORM		460	90.286
	480	Options for EXOATMOS IRRAD		420	90.440
	485	Es-roch23		460	90.561
	490	Es-roch23		420	90.610
	495	Es-roch23		460	90.693
	500	Es-roch23		420	90.731
	505	Es-roch23		460	90.742
	510	Es-roch23		420	90.742
	515	Es-roch23		460	90.742
	520	Es-roch23		420	90.742
	525	Es-roch23		460	90.742
	530	Es-roch23		420	90.742
	535	Es-roch23		460	90.742
	540	Es-roch23		420	90.742
	545	Es-roch23		460	90.742
	550	Es-roch23		420	90.742
	555	Es-roch23		460	90.742
	560	Es-roch23		420	90.742
	565	Es-roch23		460	90.742
	570	Es-roch23		420	90.742
	575	Es-roch23		460	90.742
	580	Es-roch23		420	90.742
	585	Es-roch23		460	90.742
	590	Es-roch23		420	90.742
	595	Es-roch23		460	90.742



PIXEL OUTPUT:	MONOCHROME			RAW RED (red+tr)	matrixed red (red)	RAW GREEN (green+tr)	matrixed green (green)	RAW BLUE (tr)	matrixed blue (tr)	NDVI (r-red)/(r+red)	
	SIGNAL # of e's per pixel= HAZE # of e's per pixel= Total(SIG+HAZE) # of e's per pixel=	RAW RED (red+tr)	matrixed red (red)								RAW GREEN (green+tr)
SIGNAL # of e's per pixel=	48128.14	31255.44	8804.53	18338.99	4450.38	13670.57	70803.56	0.779			
HAZE # of e's per pixel=	28522.93	10672.62	15332.85	7124.86	20851.43	10574.92	2061.09	-0.179			
Total(SIG+HAZE) # of e's per pixel=	74651.07	41888.07	24137.38	25463.85	25301.81	15731.66	81478.50	0.543			
SENSOR NOISE(e-)= 20.00											
SHOT NOISE(e-)= 273.22	204.69	155.36	20.00	20.00	20.00	20.00	20.00	20.00			
12bit QUANTIZE NOISE(e-)= 5.26	2.95	1.79	159.57	159.07	125.43	285.44	0.295				
8bit QUANTIZE NOISE(e-)= 84.18	47.25	27.22	28.71	28.53	17.74	91.88	0.543				
Total Sensor&Elec Noise # of e's per pixel=	286.64	211.04	159.00	163.38	128.25	300.59	0.308				
Grand Total # of e's per pixel=	74937.71	42109.11	24296.38	25627.22	25464.66	15859.91	81779.09	0.542			
12bit constant=	20.75										
8bit constant=	16.00										
12bit counts for SIGNAL e's= 2319											
12bit counts for HAZE e's= 1278	1505	424	884	214	659	3412	0.779				
12bit counts for Total(SIG+HAZE) e's= 3597	514	739	343	1005	99	514	-0.180				
12bit counts for Total(Sensor & Electronics)Noise e's= 14	2019	1163	1227	1219	758	3926	0.543				
12bit counts for grand total e's= 3611	10	8	8	6	14	3941	0.542				
8bit counts for SIGNAL e's=	145	94	27	55	13	41	213	0.542			
8bit counts for HAZE e's=	80	32	46	21	63	6	32	-0.179			
8bit counts for Total(SIG+HAZE) e's=	225	126	73	77	76	47	245	0.541			
8bit counts for Total(Sensor & Electronics)Noise e's=	1	1	1	1	1	0	1	0.000			
8bit counts for grand total e's=	226	127	73	77	77	48	246	0.542			
TOTAL(SIG+HAZE) Irradiance at Detector	(Watts/m <sup>2</sup> ·um <sup>2</sup> )	(g/sec·m <sup>2</sup> ·um)	M6 Q.E	M6 NORM Q.E	O.E. Norm Factor= 0.45	SIGNAL ONLY # of electrons	MONOCHROME TOTAL(SIG+HAZE) # of electrons	MONOCHROME SIGNAL ONLY # of electrons	MONOCHROME TOTAL(SIG+HAZE) # of electrons	MONOCHROME SIGNAL ONLY # of electrons	Y91 CFA-2 WAVE
0.00E+00	0.00E+00	0.175	0.07875	0	0	0	0	0	0	0	400
0.00E+00	0.00E+00	0.18	0.081	0	0	0	0	0	0	0	405
0.00E+00	0.00E+00	0.185	0.0825	0	0	0	0	0	0	0	410
0.00E+00	0.00E+00	0.155	0.06975	0	0	0	0	0	0	0	415
0.00E+00	0.00E+00	0.125	0.05625	0	0	0	0	0	0	0	420
0.00E+00	0.00E+00	0.1325	0.059625	0	0	0	0	0	0	0	425
0.00E+00	0.00E+00	0.14	0.063	0	0	0	0	0	0	0	430
0.00E+00	0.00E+00	0.175	0.07875	0	0	0	0	0	0	0	435
0.00E+00	0.00E+00	0.21	0.0945	0	0	0	0	0	0	0	440
0.00E+00	0.00E+00	0.245	0.11025	0	0	0	0	0	0	0	445
0.00E+00	0.00E+00	0.28	0.126	0	0	0	0	0	0	0	450
0.00E+00	0.00E+00	0.3	0.135	0	0	0	0	0	0	0	455
0.00E+00	0.00E+00	0.32	0.144	0	0	0	0	0	0	0	460
0.00E+00	0.00E+00	0.31	0.1395	0	0	0	0	0	0	0	465
0.00E+00	0.00E+00	0.3	0.135	0	0	0	0	0	0	0	470
0.00E+00	0.00E+00	0.295	0.13275	0	0	0	0	0	0	0	475
0.00E+00	0.00E+00	0.29	0.1305	0	0	0	0	0	0	0	480
0.00E+00	0.00E+00	0.285	0.12825	0	0	0	0	0	0	0	485
0.00E+00	0.00E+00	0.28	0.126	0	0	0	0	0	0	0	490
0.00E+00	0.00E+00	0.28	0.126	0	0	0	0	0	0	0	495
0.00E+00	0.00E+00	0.28	0.126	0	0	0	0	0	0	0	500
0.00E+00	0.00E+00	0.28	0.126	0	0	0	0	0	0	0	505
0.00E+00	0.00E+00	0.305	0.13725	0	0	0	0	0	0	0	510
0.00E+00	0.00E+00	0.33	0.1485	0	0	0	0	0	0	0	515
0.00E+00	0.00E+00	0.38	0.171	0	0	0	0	0	0	0	520
0.00E+00	0.00E+00	0.43	0.1935	0	0	0	0	0	0	0	525
0.00E+00	0.00E+00	0.48	0.216	0	0	0	0	0	0	0	530
0.00E+00	0.00E+00	0.53	0.2385	0	0	0	0	0	0	0	535
0.00E+00	0.00E+00	0.585	0.26925	0	0	0	0	0	0	0	540
0.00E+00	0.00E+00	0.64	0.288	0	0	0	0	0	0	0	545
0.00E+00	0.00E+00	0.69	0.306	0	0	0	0	0	0	0	550
0.00E+00	0.00E+00	0.74	0.333	0	0	0	0	0	0	0	555
0.00E+00	0.00E+00	0.795	0.35775	0	0	0	0	0	0	0	560
0.00E+00	0.00E+00	0.85	0.3825	0	0	0	0	0	0	0	565
0.00E+00	0.00E+00	0.885	0.39825	0	0	0	0	0	0	0	570
0.00E+00	0.00E+00	0.92	0.414	0	0	0	0	0	0	0	575
0.00E+00	0.00E+00	0.925	0.41625	0	0	0	0	0	0	0	580
0.00E+00	0.00E+00	0.93	0.4185	0	0	0	0	0	0	0	585
0.00E+00	0.00E+00	0.925	0.41625	0	0	0	0	0	0	0	590
0.00E+00	0.00E+00	0.92	0.414	0	0	0	0	0	0	0	595
0.00E+00	0.00E+00	0.925	0.41625	0	0	0	0	0	0	0	600







1.20E-01	4.38E+17	1.14E+18	0.93	0.4185	98952	495	256787	1284	600	0.302
1.24E-01	4.70E+17	1.19E+18	0.955	0.42075	106761	534	270541	1353	605	0.408
1.29E-01	4.80E+17	1.19E+18	0.94	0.423	109714	549	271741	1359	610	0.514
1.22E-01	4.94E+17	1.19E+18	0.91	0.4095	109297	546	262449	1312	615	0.5974
1.18E-01	4.98E+17	1.16E+18	0.88	0.396	106514	533	246711	1238	620	0.6808
1.13E-01	5.03E+17	1.12E+18	0.83	0.3735	101364	507	226111	1131	625	0.73755
1.16E-01	5.33E+17	1.16E+18	0.78	0.351	101003	529	219127	1096	630	0.71843
1.16E-01	5.75E+17	1.20E+18	0.755	0.33975	105571	508	221054	1105	635	0.82665
1.14E-01	5.74E+17	1.17E+18	0.73	0.3285	101865	509	207582	1038	640	0.859
1.07E-01	5.68E+17	1.16E+18	0.725	0.32625	102927	515	204806	1024	645	0.87525
1.10E+00	5.85E+17	1.10E+18	0.72	0.324	98522	493	191866	959	650	0.8995
1.06E-01	5.85E+17	1.12E+18	0.75	0.3375	106333	532	203626	1018	655	0.90785
1.06E-01	6.24E+17	1.11E+18	0.78	0.351	111587	558	210407	1052	660	0.9162
1.09E-01	6.40E+17	1.15E+18	0.815	0.36675	123641	618	227875	1140	665	0.92045
1.09E-01	6.40E+17	1.15E+18	0.85	0.3825	132209	661	238041	1190	670	0.9247
1.06E-01	6.47E+17	1.13E+18	0.875	0.39375	137614	688	239496	1197	675	0.9279
1.01E-01	6.49E+17	1.09E+18	0.9	0.405	141835	709	238070	1190	680	0.9311
9.91E-02	6.70E+17	1.07E+18	0.9	0.405	145430	732	234712	1174	685	0.93215
1.00E-01	7.17E+17	1.09E+18	0.9	0.405	156731	781	239109	1196	690	0.9332
9.76E-02	7.35E+17	1.07E+18	0.875	0.39375	156237	781	228030	1140	695	0.9343
1.03E-01	8.19E+17	1.14E+18	0.85	0.3825	169247	846	234478	1172	700	0.9354
1.14E-01	9.66E+17	1.27E+18	0.815	0.36675	191236	956	251846	1259	705	0.93755
1.22E-01	1.08E+18	1.37E+18	0.78	0.351	204885	1024	259727	1299	710	0.9397
1.24E-01	1.13E+18	1.40E+18	0.755	0.33975	207928	1040	256265	1281	715	0.94295
1.16E-01	1.13E+18	1.32E+18	0.73	0.3285	193114	966	233559	1168	720	0.9462
1.42E-01	1.39E+18	1.63E+18	0.72	0.324	242925	1215	265569	1428	725	0.9517
1.73E-01	1.73E+18	1.99E+18	0.71	0.3195	298335	1492	344023	1720	730	0.9572
2.19E-01	2.25E+18	2.54E+18	0.725	0.32625	398815	1984	447958	2240	735	0.9605
2.30E-01	2.41E+18	2.69E+18	0.74	0.333	43500	2169	484243	2421	740	0.9659
2.28E-01	2.44E+18	2.70E+18	0.77	0.3465	458869	2279	504333	2523	745	0.96715
2.66E-01	2.45E+18	2.69E+18	0.8	0.36	473338	2377	521778	2611	750	0.9705
2.32E-01	2.59E+18	2.76E+18	0.84	0.378	515169	2581	564331	2822	755	0.97385
2.24E-01	2.48E+18	2.69E+18	0.88	0.396	530010	2650	575915	2880	760	0.9772
1.81E-01	2.02E+18	2.19E+18	0.91	0.4095	445595	2228	483300	2417	765	0.98285
1.51E-01	1.70E+18	1.84E+18	0.94	0.423	388558	1943	420019	2100	770	0.9885
1.60E-01	1.81E+18	1.96E+18	0.96	0.432	422991	2115	456430	2282	775	0.99195
1.21E-01	1.39E+18	1.49E+18	0.98	0.441	330285	1651	355865	1779	780	0.9954
1.91E-02	2.21E+17	2.37E+17	0.99	0.4455	53063	265	57108	286	785	0.99655
3.31E-03	4.14E+16	4.14E+16	1	0.45	9351	47	10051	50	790	0.9977
7.75E-04	9.08E+15	9.75E+15	0.98	0.441	2163	11	2322	12	795	0.99885
1.99E-04	2.35E+15	2.52E+15	0.96	0.432	548	3	587	3	800	1
1.20E-05	1.43E+14	1.53E+14	0.94	0.423	33	0	35	0	805	1
0.00E+00	0.00E+00	0.00E+00	0.92	0.414	0	0	0	0	810	1
0.00E+00	0.00E+00	0.00E+00	0.88	0.396	0	0	0	0	815	1
0.00E+00	0.00E+00	0.00E+00	0.84	0.378	0	0	0	0	820	1
0.00E+00	0.00E+00	0.00E+00	0.835	0.37575	0	0	0	0	825	1
0.00E+00	0.00E+00	0.00E+00	0.83	0.3735	0	0	0	0	830	1
0.00E+00	0.00E+00	0.00E+00	0.83	0.3735	0	0	0	0	835	1
0.00E+00	0.00E+00	0.00E+00	0.83	0.3735	0	0	0	0	840	1
0.00E+00	0.00E+00	0.00E+00	0.825	0.37125	0	0	0	0	845	1
0.00E+00	0.00E+00	0.00E+00	0.82	0.369	0	0	0	0	850	1
0.00E+00	0.00E+00	0.00E+00	0.82	0.369	0	0	0	0	855	1
8.11E-05	1.04E+15	1.10E+15	0.82	0.369	208	1	220	1	860	1
6.16E-05	7.97E+14	8.42E+14	0.825	0.37125	160	1	169	1	865	1
3.58E-04	4.66E+15	4.93E+15	0.83	0.3735	940	5	994	5	870	1
0.00E+00	0.00E+00	0.00E+00	0.835	0.37575	0	0	0	0	875	1
1.82E-04	2.53E+15	2.67E+15	0.84	0.378	516	3	545	3	880	1
8.29E-06	1.10E+14	1.16E+14	0.83	0.3735	22	0	23	0	885	1
1.88E-04	1.85E+15	1.95E+15	0.82	0.369	369	2	388	2	890	1
2.62E-04	3.52E+15	3.71E+15	0.795	0.35775	680	3	717	4	895	1
2.24E-04	3.01E+15	3.19E+15	0.77	0.3465	563	3	596	3	900	1
0.00E+00	0.00E+00	0.00E+00	0.735	0.33075	0	0	0	0	905	1
2.42E-04	3.29E+15	3.48E+15	0.7	0.315	560	3	592	3	910	1
2.57E-04	3.53E+15	3.72E+15	0.665	0.29925	570	3	601	3	915	1
1.06E-04	1.47E+15	1.54E+15	0.63	0.2835	225	1	236	1	920	1
2.03E+00	2.13E+15	2.23E+15	0.595	0.26775	293	1	308	2	925	1
2.09E-04	2.85E+15	3.08E+15	0.56	0.252	387	2	419	2	930	1
1.13E-06	1.30E+13	1.66E+13	0.525	0.23825	2	0	2	0	935	1
4.61E-05	6.06E+14	6.86E+14	0.49	0.2205	72	0	82	0	940	1
0.00E+00	0.00E+00	0.00E+00	0.455	0.20475	0	0	0	0	945	1
3.29E-05	4.47E+14	4.94E+14	0.42	0.189	46	0	50	0	950	1
0.00E+00	0.00E+00	0.00E+00	0.395	0.17775	0	0	0	0	955	1
9.71E-05	1.40E+15	1.47E+15	0.37	0.1665	126	1	133	1	960	1
0.00E+00	0.00E+00	0.00E+00	0.345	0.15525	0	0	0	0	965	1









LOWTRAN(MOD)TRAN rootS+KM SLU-rootH+ W/m <sup>2</sup> -um-sr %	LOWTRAN(MOD)TRAN rootS+KM rootS+KM % SLU-rootH+ W/m <sup>2</sup> -um-sr %	MEASURED FILTER 650Bfilter trans	MEASURED FILTER V5filter trans	MEASURED FILTER Titina Yellow #1 trans	MEASURED FILTER hot mirror trans	MEASURED MACBETH TARGET Dark Skin reflect	MEASURED MACBETH TARGET Light Skin reflect	MEASURED MACBETH TARGET Blue Sky reflect	MEASURED MACBETH TARGET Foliage reflect
1.69E-04	2.49E+15	2.60E+15	0.32	0.144	194	1	202	218	970
1.94E-04	2.99E+15	2.99E+15	0.3	0.135	209	1	218	975	1
1.29E-04	1.99E+15	1.99E+15	0.28	0.126	130	0	136	980	1
0.00E+00	0.00E+00	0.00E+00	0.255	0.11475	0	0	0	985	1
2.48E-04	3.75E+15	3.89E+15	0.23	0.1035	210	1	217	990	1
0.00E+00	0.00E+00	0.00E+00	0.215	0.09675	0	0	0	995	1
7.95E-05	1.21E+15	1.26E+15	0.19	0.0855	56	0	58	1000	1

MEASURED MACBETH TARGET Blow Flower	MEASURED MACBETH TARGET Bluish Green		MEASURED MACBETH TARGET Orange		MEASURED MACBETH TARGET Purplish Blue		MEASURED MACBETH TARGET Moderate Red		MEASURED MACBETH TARGET Yellow		MEASURED MACBETH TARGET Orange Yr Green		MEASURED MACBETH TARGET Green		MEASURED MACBETH TARGET Red		MEASURED MACBETH TARGET Yellow		MEASURED MACBETH TARGET Magenta		MEASURED MACBETH TARGET Cyan		MEASURED MACBETH TARGET White		MEASURED MACBETH TARGET Neutral 6.5		MEASURED MACBETH TARGET Neutral 5			
	reflect	reflect	reflect	reflect	reflect	reflect	reflect	reflect	reflect	reflect	reflect	reflect	reflect	reflect	reflect	reflect	reflect	reflect	reflect	reflect	reflect	reflect	reflect	reflect	reflect	reflect	reflect	reflect	reflect	
0.895	0.87	155	182	1	139	1	145	1	135	1	141	1	146	1	141	1	146	1	135	1	141	1	146	1	135	1	141	1	146	1
0.895	0.87	168	175	1	150	1	156	1	156	1	152	1	146	1	152	1	146	1	156	1	152	1	146	1	156	1	152	1	146	1
0.895	0.87	104	108	1	93	0	97	0	97	0	94	0	91	0	94	0	91	0	97	0	94	0	91	0	97	0	94	0	91	0
0.895	0.87	0	0	0	0	0	0	0	0	0	0	0	0	0	0	0	0	0	0	0	0	0	0	0	0	0	0	0	0	0
0.895	0.87	168	174	1	150	1	156	1	156	1	151	1	146	1	151	1	146	1	156	1	151	1	146	1	156	1	151	1	146	1
0.895	0.87	0	0	0	0	0	0	0	0	0	0	0	0	0	0	0	0	0	0	0	0	0	0	0	0	0	0	0	0	0
0.895	0.87	45	46	0	40	0	42	0	42	0	39	0	39	0	40	0	39	0	42	0	39	0	39	0	42	0	39	0	39	0

MEASURED WACBETH-TARE Neutral 3.5 reflect	MEASURED WACBETH-TARE reflect	MEASURED WHEAT reflect	MEASURED WHEAT-NEW reflect	MEASURED WHEAT-NORM reflect	for lab test Light Source BB-5800 (Watts/m <sup>2</sup> ·µr)	for lab test Light Source BB-5800 (Watts/m <sup>2</sup> ·µr)	for lab test Light Source D65 (Watts/m <sup>2</sup> ·µr)	for lab test for lab test LAB-TRANS LAB-TRANS (%)	#VALUE! #VALUE! #VALUE!	#VALUE! #VALUE! #VALUE!	#VALUE! #VALUE! #VALUE!
0.77465338	1.11041295	1.27625616	-1.36154422	-0.75623449	3.49056061	0.80793908	1.15812573	1.33109499	-1.42004774	-0.78872876	3.64054479
0.83773398	1.20083469	1.38018265	-1.47241577	-0.81781522	3.77479954	0.87310749	1.25154021	1.43846117	-1.53458886	-0.85234766	3.9341913
0.52101706	0.74684253	0.85838551	-0.91574863	-0.50862887	2.34758437	0.54202661	0.77695829	0.89298914	-0.85267538	-0.52913887	2.44235265
0.83817676	1.20146939	1.38091214	-1.47319402	-0.81824748	3.7767947	0.86982208	1.24654412	1.43271891	-1.52846286	-0.84894513	3.91848621
0.224002958	0.32109246	0.3690485	-0.39371082	-0.21867648	1.00934766	0.23207589	0.332866501	0.38234944	-0.40790061	-0.22555784	1.04572572
9.2900	3.8500	6.000	5.000	4.000				33.045065			
9.3300	3.8600	6.000	5.100	4.200				100			
9.3500	3.8500	6.000	5.200	4.300				100			
9.4500	3.8500	6.000	5.300	4.500				100			
9.6100	3.8500	6.000	5.400	4.600				100			
9.5500	3.8500	6.100	5.500	4.700				100			
9.5900	3.8200	6.100	5.600	4.800				100			
9.6500	3.8000	6.100	5.600	4.900				100			
9.6400	3.8000	6.000	5.600	5.000				100			
9.7300	3.8100	6.000	5.600	5.000				100			
9.6800	3.8400	6.000	5.500	5.000				100			
9.5900	3.8100	6.000	5.300	4.900				100			
9.5600	3.7900	5.900	5.100	4.800				100			
9.4800	3.7600	5.900	5.000	4.700				100			
9.4400	3.7500	5.900	4.900	4.700				100			
9.4000	3.7600	5.800	4.800	4.600				100			
9.4000	3.7700	5.800	4.800	4.600				100			
9.4000	3.8000	5.900	4.800	4.700				100			
9.3800	3.7700	5.800	4.800	4.700				100			
9.3500	3.7500	5.800	4.800	4.700				100			
9.3500	3.7000	6.000	5.900	5.000				100			
9.3500	3.7000	6.000	6.000	6.000				100			
9.3400	3.7000	6.000	6.000	6.000				100			
9.3400	3.7000	6.000	7.100	7.100				100			
9.3400	3.7000	7.000	7.500	7.400				100			
9.3400	3.7000	7.000	7.500	7.500				100			
9.3400	3.7000	7.000	7.900	7.500				100			
9.3300	3.7000	7.000	8.000	7.500				100			
9.3400	3.7000	7.000	8.000	7.500				100			
9.4100	3.7000	6.700	7.900	7.400				100			
9.4100	3.7000	6.500	7.500	7.400				100			
9.4400	3.7000	6.200	7.200	7.300				100			
9.4700	3.6700	6.000	6.800	7.300				100			
9.5000	3.6700	5.700	6.400	7.200				100			
9.5000	3.6900	5.500	6.000	7.200				100			
9.4900	3.6800	5.300	5.600	7.100				100			
9.4900	3.6800	5.100	5.300	7.100				100			
9.4500	3.6700	5.000	5.000	7.000				100			
9.4400	3.7000	5.000	4.800	6.900				100			
9.4000	3.6900	5.000	4.700	6.800				100			
9.3800	3.7000	5.100	4.700	6.800				100			
9.2900	3.7000	5.200	4.800	6.600				100			
9.2900	3.7000	5.400	5.000	6.500				100			
9.2400	3.7000	5.500	5.200	6.400				100			
9.2000	3.7000	5.700	5.500	6.200				100			
9.1600	3.7100	5.800	5.900	6.000				100			
9.1200	3.7200	5.900	6.400	5.800				100			
9.1000	3.7500	6.000	7.000	5.500				100			
9.0400	3.7500	6.000	7.000	5.200				100			
9.0300	3.7500	6.100	8.300	4.900				100			
8.9900	3.7800	6.200	9.900	4.400				100			
8.9600	3.7900	6.500	11.000	4.300				100			
8.9100	3.8000	6.900	12.000	4.400				100			
8.9000	3.8000	7.500	13.000	4.600				100			
8.8000	3.8000	8.400	14.000	5.000				100			
8.8500	3.8000	9.500	14.000	5.600				100			
8.8200	3.8100	11.000	15.000	6.500				100			



0.01057812	36.3111	12.6603	0.798226761	88.50	87.34	32.1000	75.7400	10.7500	29.2400
0.00937674	13.4844	55.05619049	0.609517097	88.43	87.44	33.5500	77.4800	10.7400	32.6400
0.00791317	35.6274	53.86133194	0.537095533	88.50	87.85	35.2800	79.0700	10.7000	35.1200
0.01332684	21.0415	54.25987108	0.486615036	88.33	87.06	37.9900	80.3700	10.7100	36.7800
0.01376297	22.3596	55.86709512	0.38455227	88.26	85.36	39.7500	81.5700	10.7000	37.8500
0.01267848	26.2682	61.03233152	0.247457359	88.07	84.22	42.2400	82.8900	10.7000	38.5800
0.01215805	35.7907	61.26401138	0.141259166	88.05	84.31	44.7100	83.9800	10.7000	39.0800
0.01198896	41.855	65.8584137	0.076320503	87.86	84.25	47.1400	84.0500	10.7100	39.4800
0.01270682	44.7459	60.24274826	0.050354004	87.88	84.35	49.4000	84.6800	10.7600	39.8700
0.01268683	39.4498	57.41860867	0.040435791	87.87	84.59	51.5600	85.0400	10.8000	40.1900
0.01282838	29.1166	56.46102428	0.035119057	87.69	84.59	53.8800	85.3900	10.8000	40.5100
0.01207098	46.4026	52.9178381	0.050139427	87.56	84.04	54.7900	85.7400	10.8000	40.8700
0.01250683	46.6197	43.6013055	0.073027611	87.43	84.33	55.7100	85.9300	10.9100	41.1500
0.01274073	42.8108	36.30588055	0.069308281	87.30	84.88	56.1200	86.1100	10.9600	41.4800
0.01139894	42.8108	40.8622169	0.068664551	87.36	86.31	56.3100	86.2200	11.0300	41.8000
0.01285751	42.8108	30.06985188	0.047445297	87.19	86.55	56.0400	86.4000	11.1100	42.1300
0.01139894	42.8108	4.770207405	0.009942055	87.01	86.55	56.0400	86.5100	11.1900	42.4900
0.01224682	40.8419	0.850582123	-0.013279915	87.12	86.98	55.6500	86.5200	11.2500	42.8200
0.01139894	9.2381	0.209999084	-0.002813339	86.98	86.98	55.1600	86.5400	11.3400	43.1000
0.01266411	43.6253	0.053858757	-0.016403198	86.78	86.78	54.7300	86.5900	11.4400	43.4500
0.01168376	30.7838	0.003333786	0.004959106	86.65	86.65	54.2200	86.6500	11.5600	43.7400
0.01168376	31.0025	0	-0.019955635	86.34	86.34	53.7600	86.7500	11.6200	44.1000
0.01168376	33.3876	0	0.000739098	86.67	86.67	52.8100	86.8400	11.7500	44.4700
0.00970379	39.2812	0	0.069284439	86.51	86.51	52.5500	86.9300	11.8400	44.7700
0.01213456	45.2096	0	0.172710419	86.31	86.31	52.1300	86.9900	12.0400	45.3900
0.01195366	48.0618	0	0.459074974	86.08	86.08	51.7900	86.9400	12.1600	45.6800
0.0082977	49.0582	0	0.779140572	86.06	86.06	51.7900	86.9400	12.1600	45.6800
0.01153953	49.4304	0	0.044441223	85.91	85.91	51.7900	86.9400	12.1600	45.6800
0.01110309	50.8309	0	-0.008274483	86.27	86.27	51.5200	86.8100	12.3000	46.0600
0.01104999	50.8723	0	-0.16951561	86.01	86.01	51.3900	86.8700	12.3000	46.2500
0.00983925	49.9301	0	-0.162434578	85.72	85.72	51.3900	86.4900	12.0500	46.4600
0.01142126	39.1339	0	0.333142281	85.56	85.56	51.0000	86.8900	11.9000	46.1000
0.01051148	24.6988	0.064563751	0.65504055	85.61	85.61	50.9700	86.6200	11.3600	46.3300
0.01013584	23.1197	0.03027916	0.134921074	85.46	85.46	51.2300	87.0200	11.7600	46.7000
0.0105806	27.4413	0.051808357	0.887146187	85.67	85.67	51.3800	86.8800	12.3700	46.9900
0.01099669	22.3885	0.114345551	3.08535099	85.65	85.65	52.2200	86.9400	12.6900	47.1100
0.01083475	1.09027	0.129055977	2.501749992	85.61	85.61	52.4000	87.0200	12.9000	47.4500
0.01058991	3.01269	0	0	85.14	85.14	53.6700	87.9000	13.8100	47.5900
0.01024688	5.16036	0	0.13666153	85.02	85.02	54.2800	87.9000	14.1000	47.6600
0.00940024	13.9429	0	0.137066841	85.31	85.31	54.9500	87.2600	14.4600	48.0500
0.01038102	30.18	0	0.051164627	84.97	84.97	55.7300	87.9400	14.7500	48.1800
0.0099732	38.2997	0	0.07724762	85.27	85.27	56.5500	87.5500	15.0800	48.3000
0.00959603	53.142	0	0.3452921536	84.88	84.88	57.3800	87.2900	15.3400	48.4400
0.00959603	53.142	0	0.166860035	85.08	85.08	58.2000	87.5100	15.6200	48.6800
0.00959603	53.142	0	0.239419337	85.05	85.05	60.0600	87.4900	15.9800	48.7900
0.00940024	13.9429	0	0.110292435	84.92	84.92	61.0600	87.4900	16.3700	48.8900
0.01038102	30.18	0	0.087165833	85.36	85.36	62.0200	87.5500	16.7600	49.0600
0.0099732	38.2997	0	0.092840195	85.12	85.12	62.8500	87.6300	17.1600	49.1700
0.00959603	53.142	0	0.108408928	84.84	84.84	64.0100	87.6400	17.5500	49.2500
0.00959603	53.142	0	0.065588951	84.74	84.74	64.8600	87.6900	18.4300	49.4000
0.00959603	53.142	0	0.115776062	84.89	84.89	65.8600	87.6900	18.8600	49.5400
0.00959603	53.142	0	0	84.69	84.69	66.7300	87.6800	19.3600	49.6000
0.00940024	13.9429	0	0.037433171	84.74	84.74	68.4100	87.7100	20.4000	49.6300
0.00940024	13.9429	0	0	84.64	84.64	69.1200	87.7400	20.9200	49.6600
0.00940024	13.9429	0	0	84.53	84.53	70.4400	87.7200	21.4900	49.7100
0.00940024	13.9429	0	0	84.53	84.53	70.4400	87.6900	22.0200	49.6800



8.8000	3.8000	13.0000	16.0000	7.7000	100	34.238096
8.7600	3.8000	15.0000	17.0000	9.1000	100	34.143411
8.7500	3.8100	17.0000	17.0000	11.0000	100	34.048726
8.7100	3.8000	20.0000	13.0000	13.0000	100	33.878293
8.7000	3.8200	23.0000	19.0000	15.0000	100	33.745734
8.6600	3.8300	25.0000	19.0000	17.0000	100	33.632112
8.6100	3.8500	28.0000	20.0000	19.0000	100	33.499553
8.7000	3.8500	30.0000	21.0000	21.0000	100	33.385931
8.6200	3.8600	32.0000	21.0000	23.0000	100	33.291246
8.5900	3.8800	34.0000	22.0000	25.0000	100	33.13975
8.5600	3.8600	35.0000	23.0000	27.0000	100	33.026128
8.5200	3.8600	37.0000	23.0000	29.0000	100	32.95038
8.5700	3.8900	37.0000	24.0000	30.0000	100	32.836758
8.4800	3.8900	38.0000	24.0000	32.0000	100	32.749262
8.4500	3.8800	38.0000	25.0000	33.0000	100	32.685262
8.3700	3.8900	38.0000	25.0000	34.0000	100	32.57164
8.4000	3.9000	38.0000	26.0000	35.0000	100	32.439081
8.3700	3.8900	38.0000	26.0000	36.0000	100	32.306522
8.3500	3.9100	38.0000	27.0000	37.0000	100	32.249711
8.5900	3.8900	38.0000	27.0000	38.0000	100	32.136089
8.3400	3.8900	38.0000	27.0000	39.0000	100	32.00353
8.3200	3.9000	38.0000	27.0000	39.0000	100	31.946719
8.2900	3.9000	38.0000	28.0000	39.0000	100	31.795223
8.2900	3.9000	37.0000	28.0000	40.0000	100	31.700538
8.2800	3.9000	37.0000	28.0000	40.0000	100	31.567579
8.2300	3.8900	37.0000	28.0000	40.0000	100	31.43542
8.2000	3.8400	37.0000	28.0000	40.0000	100	31.302861
8.1500	3.8400	37.0000	28.0000	40.0000	100	31.170302
8.0900	3.7500	37.0000	28.0000	40.0000	100	31.037743
8.0400	3.6500	37.0000	28.0000	40.0000	100	30.905184
8.0400	3.6200	37.0000	28.0000	40.0000	100	30.772625
5.1600	2.8900	37.0000	28.0000	40.0000	100	30.640066
6.1100	1.8500	37.0000	28.0000	40.0000	100	30.507507
6.3200	2.1100	37.0000	28.0000	40.0000	100	30.374948
6.4200	2.2600	37.0000	28.0000	40.0000	100	30.242389
6.5700	2.2400	37.0000	28.0000	40.0000	100	30.109830
7.0000	2.5300	37.0000	28.0000	40.0000	100	29.977271
6.8700	2.5100	37.0000	28.0000	40.0000	100	29.844712
7.0800	2.7700	37.0000	28.0000	40.0000	100	29.712153
7.1100	2.8000	37.0000	28.0000	40.0000	100	29.579594
7.0700	2.8800	37.0000	28.0000	40.0000	100	29.447035
7.1500	2.8200	37.0000	28.0000	40.0000	100	29.314476
7.2600	2.8000	37.0000	28.0000	40.0000	100	29.181917
7.2900	2.8800	37.0000	28.0000	40.0000	100	29.049358
7.3200	3.0200	37.0000	28.0000	40.0000	100	28.916799
7.2700	3.0500	37.0000	28.0000	40.0000	100	28.784240
7.3200	2.9900	37.0000	28.0000	40.0000	100	28.651681
7.2600	3.0600	37.0000	28.0000	40.0000	100	28.519122
7.3700	3.1100	37.0000	28.0000	40.0000	100	28.386563
7.3600	3.1400	37.0000	28.0000	40.0000	100	28.254004
7.3800	3.0700	37.0000	28.0000	40.0000	100	28.121445
7.3500	3.1200	37.0000	28.0000	40.0000	100	27.988886
7.3500	3.1100	37.0000	28.0000	40.0000	100	27.856327
7.3300	3.1000	37.0000	28.0000	40.0000	100	27.723768
7.3100	3.1200	37.0000	28.0000	40.0000	100	27.591209
7.3400	3.1100	37.0000	28.0000	40.0000	100	27.458650
7.3100	3.1300	37.0000	28.0000	40.0000	100	27.326091
7.3300	3.1000	37.0000	28.0000	40.0000	100	27.193532
7.3200	3.1000	37.0000	28.0000	40.0000	100	27.060973

**Appendix 4 - Image Quality Model Sample Run**





MEASURED		DETECTOR/FPA MTF												combo	
TOTAL		LENS		clockMTF		detectorMTF		x-transMTF		total		total		electronic	
QF	MTF	FREQ (lp/mm)	IN-TRK	IN-TRK	BOTH	IN-TRK	IN-TRK	X-TRK	X-TRK	fpaMTF	IN-TRK	fpaMTF	X-TRK	MTF	BOTH
1.000	1.000	0.00	1.0000	1.0000	1.0000	1.0000	1.0000	1.0000	1.0000	1.0000	1.0000	1.0000	1.0000	1.000	1.000
1.000	0.958	5.00	0.9992	0.9967	0.9992	0.9967	0.9992	0.9992	0.9988	0.9950	0.9950	0.9955	0.9955	1.000	1.000
1.000	0.909	10.00	0.9967	0.9867	0.9867	0.9968	0.9968	0.9952	0.9803	0.9820	0.9820	0.9820	0.9820	1.000	1.000
1.000	0.850	15.00	0.9925	0.9703	0.9703	0.9931	0.9931	0.9897	0.9564	0.9603	0.9603	0.9603	0.9603	1.000	1.000
1.000	0.789	20.00	0.9867	0.9475	0.9475	0.9883	0.9883	0.9826	0.9240	0.9310	0.9310	0.9310	0.9310	1.000	1.000
1.000	0.724	25.00	0.9793	0.9188	0.9188	0.9829	0.9829	0.9745	0.8844	0.8954	0.8954	0.8954	0.8954	1.000	1.000
1.000	0.653	30.00	0.9703	0.8843	0.8843	0.9772	0.9772	0.9662	0.8385	0.8544	0.8544	0.8544	0.8544	1.000	1.000
1.000	0.590	35.00	0.9597	0.8446	0.8446	0.9718	0.9718	0.9581	0.7877	0.8092	0.8092	0.8092	0.8092	1.000	1.000
1.000	0.525	40.00	0.9475	0.8000	0.8000	0.9670	0.9670	0.9511	0.7331	0.7609	0.7609	0.7609	0.7609	1.000	1.000
1.000	0.468	45.00	0.9339	0.7512	0.7512	0.9633	0.9633	0.9456	0.6758	0.7104	0.7104	0.7104	0.7104	1.000	1.000
1.000	0.418	50.00	0.9188	0.6986	0.6986	0.9608	0.9608	0.9420	0.6168	0.6582	0.6582	0.6582	0.6582	1.000	1.000
1.000	0.375	55.00	0.9022	0.6430	0.6430	0.9599	0.9599	0.9406	0.5568	0.6048	0.6048	0.6048	0.6048	1.000	1.000
1.000	0.338	60.00	0.8843	0.5848	0.5848	0.9605	0.9605	0.9415	0.4967	0.5506	0.5506	0.5506	0.5506	1.000	1.000
1.000	0.305	65.00	0.8651	0.5248	0.5248	0.9626	0.9626	0.9447	0.4371	0.4958	0.4958	0.4958	0.4958	1.000	1.000
1.000	0.279	70.00	0.8446	0.4637	0.4637	0.9661	0.9661	0.9498	0.3784	0.4404	0.4404	0.4404	0.4404	1.000	1.000
1.000	0.256	75.00	0.8229	0.4021	0.4021	0.9707	0.9707	0.9565	0.3212	0.3846	0.3846	0.3846	0.3846	1.000	1.000
1.000	0.236	80.00	0.8000	0.3406	0.3406	0.9760	0.9760	0.9643	0.2660	0.3285	0.3285	0.3285	0.3285	1.000	1.000
1.000	0.220	85.00	0.7761	0.2800	0.2800	0.9816	0.9816	0.9727	0.2133	0.2724	0.2724	0.2724	0.2724	1.000	1.000

INTERPOLATION		PIXELTYPE-> GREEN		AIRCRAFT MOTION MTF		LINEAR MOTION SMEAR		IN-TRK	X-TRK
RED PIXEL	GREEN PIXEL	BLUE PIXEL		smr amt(um)=	equal pixel amt =	IN-TRK	X-TRK	smr amt(um)=	equal pixel amt =
interp	interp	interp	interp	IN-TRK	IN-TRK	system	system	IN-TRK	X-TRK
green	red or blue	interp	interp	smear MTF	smear MTF	smear MTF	smear MTF	smear MTF	smear MTF
MTF	MTF	BOTH	BOTH	IN-TRK	IN-TRK	IN-TRK	IN-TRK	IN-TRK	X-TRK
1.0000	1.0000	1.0000	1.0000	1.0000	1.0000	1.0000	1.0000	1.0000	1.0000
0.9901	1.0244	0.9901	0.9901	0.9787	0.9787	0.9787	0.9787	0.9787	0.9787
0.9611	1.0912	0.9611	0.9611	0.9166	0.9166	0.9166	0.9166	0.9166	0.9166
0.9153	1.1830	0.9153	0.9153	0.8182	0.8182	0.8182	0.8182	0.8182	0.8182
0.8564	1.2765	0.8564	0.8564	0.6910	0.6910	0.6910	0.6910	0.6910	0.6910
0.7891	1.3493	0.7891	0.7891	0.5445	0.5445	0.5445	0.5445	0.5445	0.5445
0.7187	1.3867	0.7187	0.7187	0.3891	0.3891	0.3891	0.3891	0.3891	0.3891
0.6507	1.3852	0.6507	0.6507	0.2358	0.2358	0.2358	0.2358	0.2358	0.2358
0.5906	1.3531	0.5906	0.5906	0.0946	0.0946	0.0946	0.0946	0.0946	0.0946
0.5432	1.3074	0.5432	0.5432	-0.0259	-0.0259	-0.0259	-0.0259	-0.0259	-0.0259
0.5122	1.2678	0.5122	0.5122	-0.1194	-0.1194	-0.1194	-0.1194	-0.1194	-0.1194
0.5001	1.2502	0.5001	0.5001	-0.1821	-0.1821	-0.1821	-0.1821	-0.1821	-0.1821
0.5079	1.2615	0.5079	0.5079	-0.2131	-0.2131	-0.2131	-0.2131	-0.2131	-0.2131
0.5348	1.2974	0.5348	0.5348	-0.2143	-0.2143	-0.2143	-0.2143	-0.2143	-0.2143
0.5789	1.3434	0.5789	0.5789	-0.1901	-0.1901	-0.1901	-0.1901	-0.1901	-0.1901
0.6365	1.3802	0.6365	0.6365	-0.1466	-0.1466	-0.1466	-0.1466	-0.1466	-0.1466
0.7032	1.3896	0.7032	0.7032	-0.0910	-0.0910	-0.0910	-0.0910	-0.0910	-0.0910
0.7735	1.3610	0.7735	0.7735	-0.0311	-0.0311	-0.0311	-0.0311	-0.0311	-0.0311

ATMOS MTF		bit MTF		total atmos		ITM		total sys	
v(lp/cm)	BOTH	BOTH	BOTH	BOTH	BOTH	mtf	mtf	mtf	mtf
0.00	1.000	1.000	1.000	1.000	1.000	0.00	1.000	1.000	1.000
5.00	1.000	1.000	1.000	1.000	1.000	5.00	0.292	0.292	0.298
10.00	1.000	1.000	1.000	1.000	1.000	10.00	0.259	0.259	0.283
15.00	1.000	1.000	1.000	1.000	1.000	15.00	0.217	0.217	0.265
20.00	1.000	1.000	1.000	1.000	1.000	20.00	0.170	0.170	0.246
25.00	1.000	1.000	1.000	1.000	1.000	25.00	0.123	0.123	0.225
30.00	1.000	1.000	1.000	1.000	1.000	30.00	0.079	0.079	0.203
35.00	1.000	1.000	1.000	1.000	1.000	35.00	0.043	0.043	0.184
40.00	1.000	1.000	1.000	1.000	1.000	40.00	0.015	0.015	0.163
45.00	1.000	1.000	1.000	1.000	1.000	45.00	-0.004	-0.004	0.146
50.00	1.000	1.000	1.000	1.000	1.000	50.00	-0.016	-0.016	0.130
55.00	1.000	1.000	1.000	1.000	1.000	55.00	-0.021	-0.021	0.117
60.00	1.000	1.000	1.000	1.000	1.000	60.00	-0.022	-0.022	0.105
65.00	1.000	1.000	1.000	1.000	1.000	65.00	-0.020	-0.020	0.095
70.00	1.000	1.000	1.000	1.000	1.000	70.00	-0.017	-0.017	0.087
75.00	1.000	1.000	1.000	1.000	1.000	75.00	-0.012	-0.012	0.080
80.00	1.000	1.000	1.000	1.000	1.000	80.00	-0.007	-0.007	0.073
85.00	1.000	1.000	1.000	1.000	1.000	85.00	-0.002	-0.002	0.068

NDVI	
background	0.407
target	0.775
<b>target</b>	
<b>contrast =</b>	<b>1.90418</b>
MODtarget=	0.311











90.00	1.000	1.000	1.000	1.000	1.000	90.00	0.002	0.064
95.00	1.000	1.000	1.000	1.000	1.000	95.00	0.004	0.060
100.00	1.000	1.000	1.000	1.000	1.000	100.00	0.006	0.056
105.00	1.000	1.000	1.000	1.000	1.000	105.00	0.007	0.053
110.00	1.000	1.000	1.000	1.000	1.000	110.00	0.006	0.049
115.00	1.000	1.000	1.000	1.000	1.000	115.00	0.005	0.045
120.00	1.000	1.000	1.000	1.000	1.000	120.00	0.004	0.042
125.00	1.000	1.000	1.000	1.000	1.000	125.00	0.002	0.038



**Appendix 5 - Image Processing Diagram**

## CIR Camera Image Processing

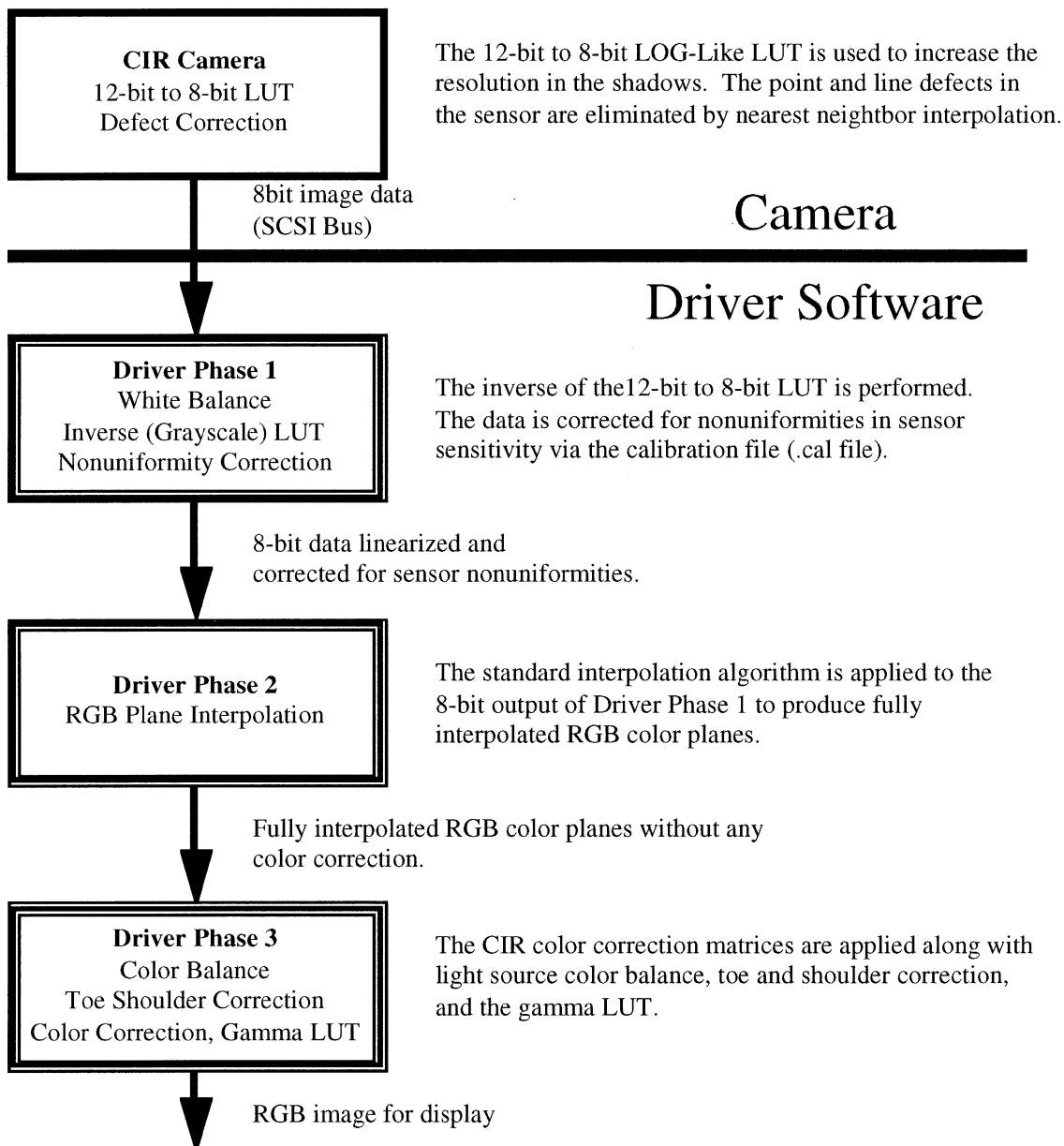


Figure 25: The CIR Camera Image Processing Diagram

## 7.0 References

1. Adams, J.E. Jr. (1997). *Design of practical color filter array interpolation algorithms for digital cameras*, Eastman Kodak Company, Imaging Research and Advanced Development, Rochester, NY 14653-5408
2. Boyd, R.W. (1983). *Radiometry and the Detection of Optical Radiation*, Wiley, NY.
3. Brainard, K. H. (1994). *Bayesian Method for Reconstructing Color Images from Trichromatic Samples*, Proceedings, IS&T's 47th Annual Conference/ICPS, 375-380 .
4. Dereniak, E.L. & Crowe, D.G. (1984). *Optical Radiation Detectors*, Wiley, NY.
5. Eastman Kodak Company, *Aerial Data, Kodak Aerochrome II Infrared Film 2443...*, Kodak Pub. AS-69, 12/96
6. Eastman Kodak Company, *Kodak Digital Science Color Infrared Cameras*, Publication : AS-902, 7/97.
7. Eastman Kodak Company, *KAF - 6300 Full-Frame CCD Image Sensor Performance Specification*, Rev. 0 , April 29, 1993.
8. Eastman Kodak Company, *KODAK Professional DCS 420 Digital Camera System - Programmer's Reference Manual* Models: DCS 420m, 420c, September, 1994.
9. Ekiert, S. E., *Threshold Modulation Equation for CCD Imagers*, paper presented at the Optical Society of America, 1979 Annual Meeting, Rochester, NY, 9 - 12 October 1979
10. Gaskill, J.D. (1978). *Linear Systems, Fourier Transforms, and Optics*, Wiley, NY.
11. Goodman, J.W. (1968). *Introduction to Fourier Optics*, McGraw-Hill, NY.
12. Parulski, K.A (1985). *Color Filters and Processing Alternatives for One Chip Camera*, IEEE Trans. Electron Devices, ED-32, 1381-1389
13. Schott, J. R. (1997). *Remote Sensing: The Image Chain Approach*, Oxford, NY.
14. Smith, W.J. (1966). *Modern Optical Engineering*, McGraw-Hill, NY.
15. Tantalo, F.J. (1996). *Modeling the MTF and Noise Characteristics of an Image Chain for a Synthetic Image Generation System*, M.S. Thesis, Rochester Institute of Technology.

